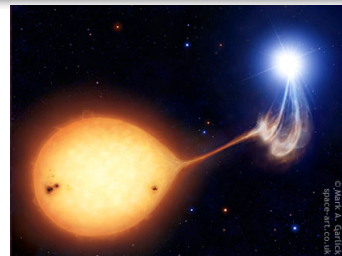
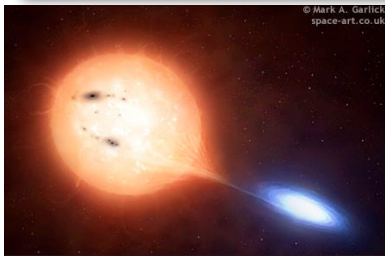
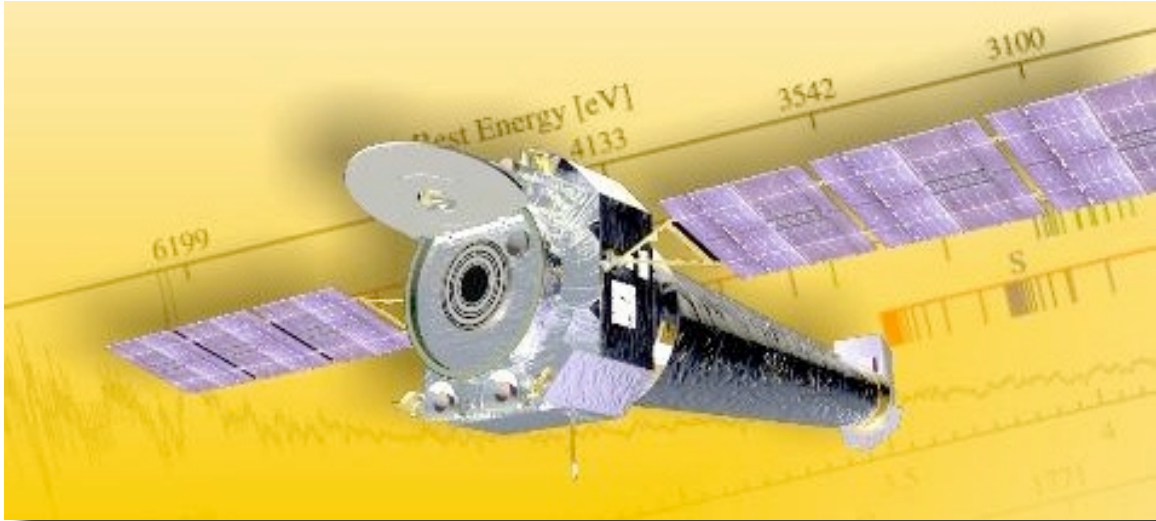


X-ray Grating Spectroscopy of Cataclysmic Variables



Christopher Mauche

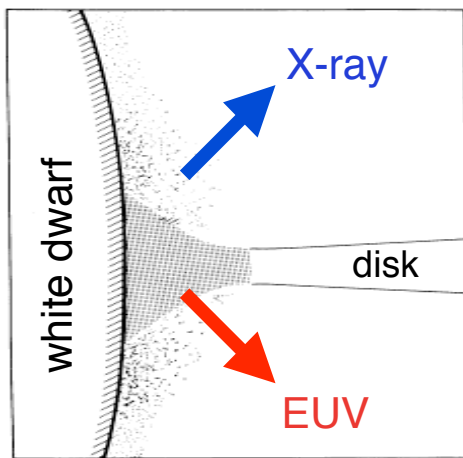
Lawrence Livermore National Laboratory



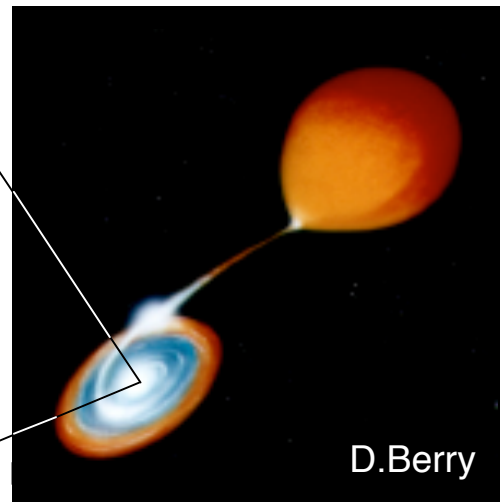
X-ray Grating Spectroscopy • Cambridge, MA • 2007 July 11–13

Accretion geometry and X-ray emission regions of nonmagnetic CVs & polars

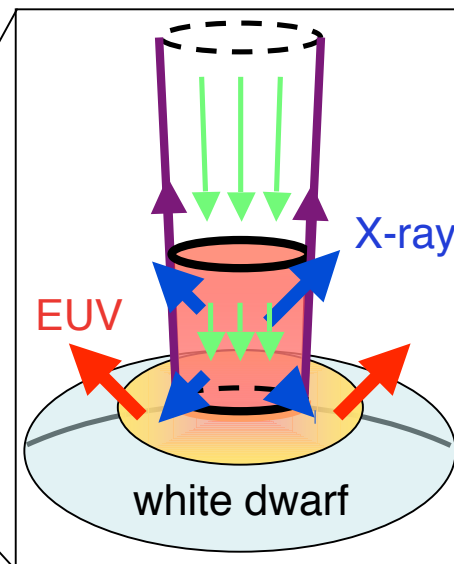
Nonmagnetic CV (dwarf nova, novalike variable)



Patterson & Raymond (1985)

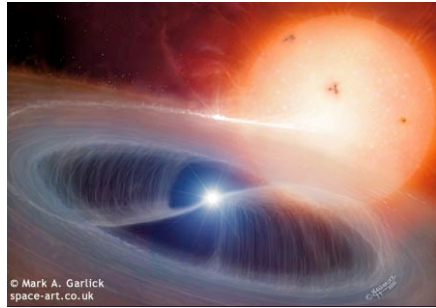


Magnetic CV (polar)

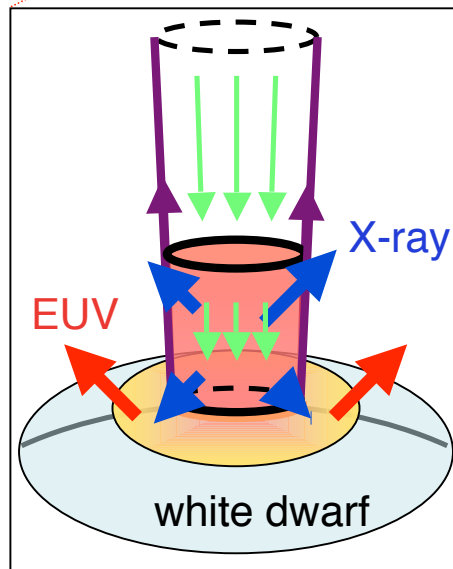
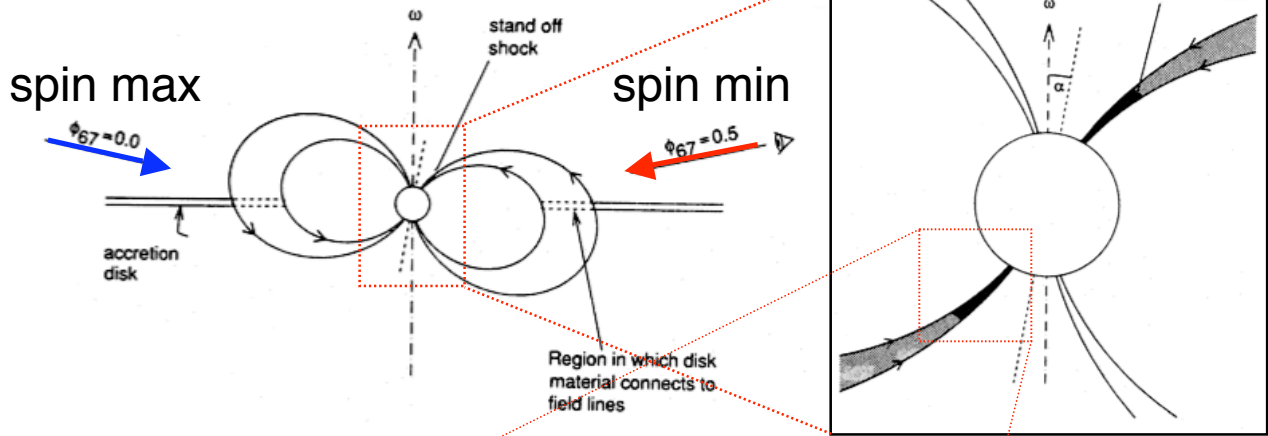


V. Burwitz

Accretion geometry and X-ray emission regions of intermediate polars (EX Hya)



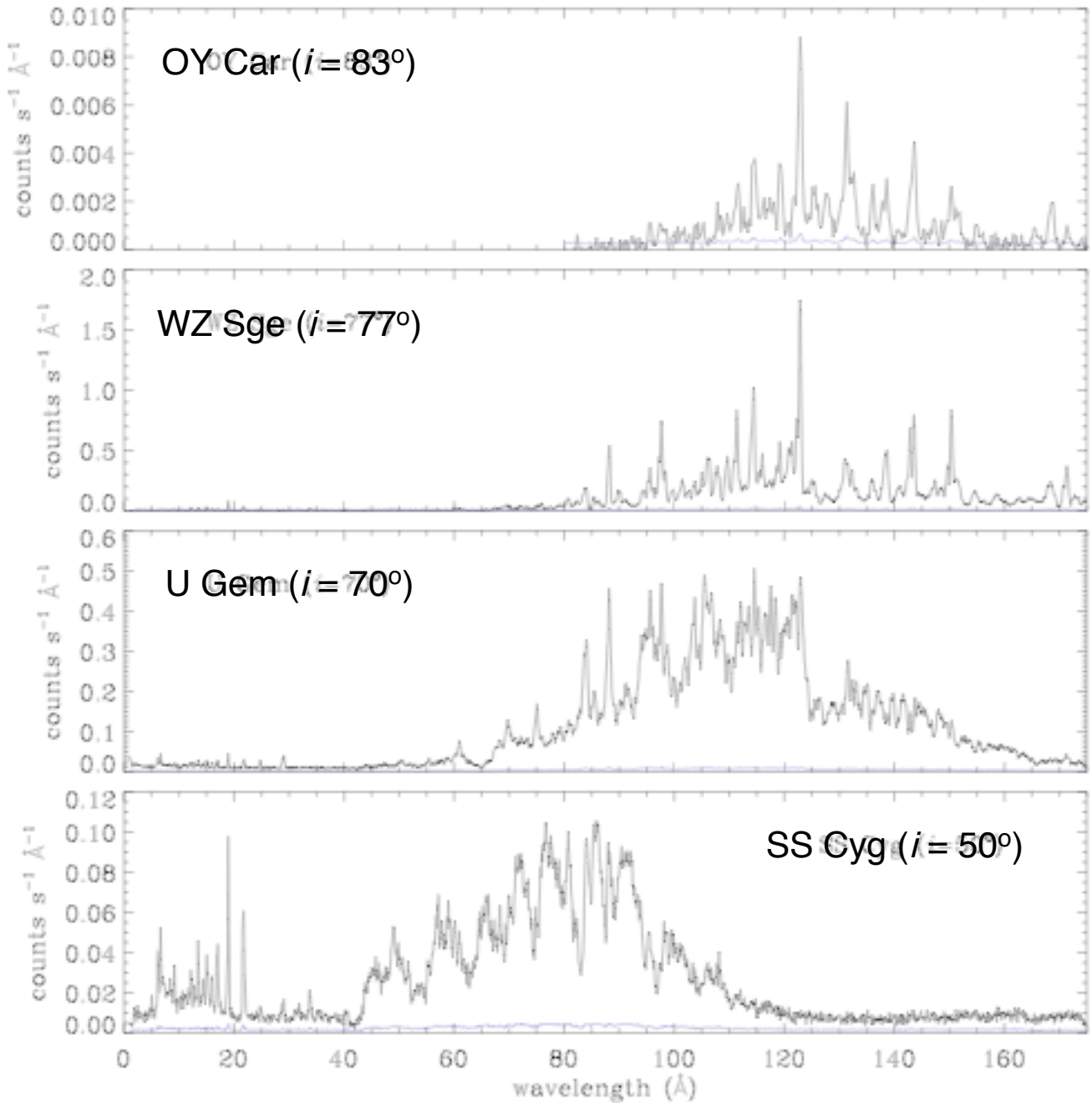
M.Garlick



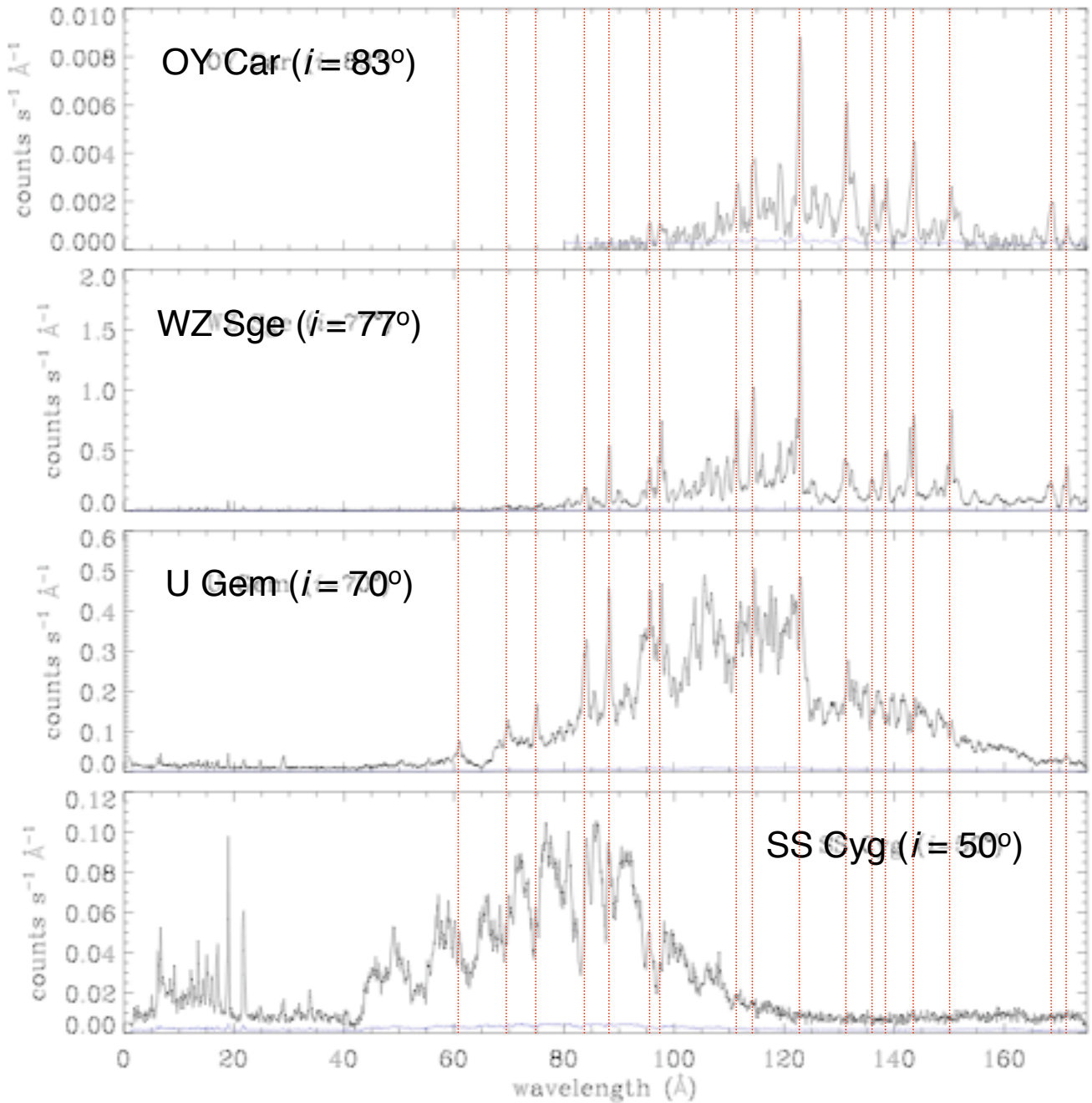
V.Burwitz

Hellier et al. (1987); Rosen, Mason, & Córdoba (1988)

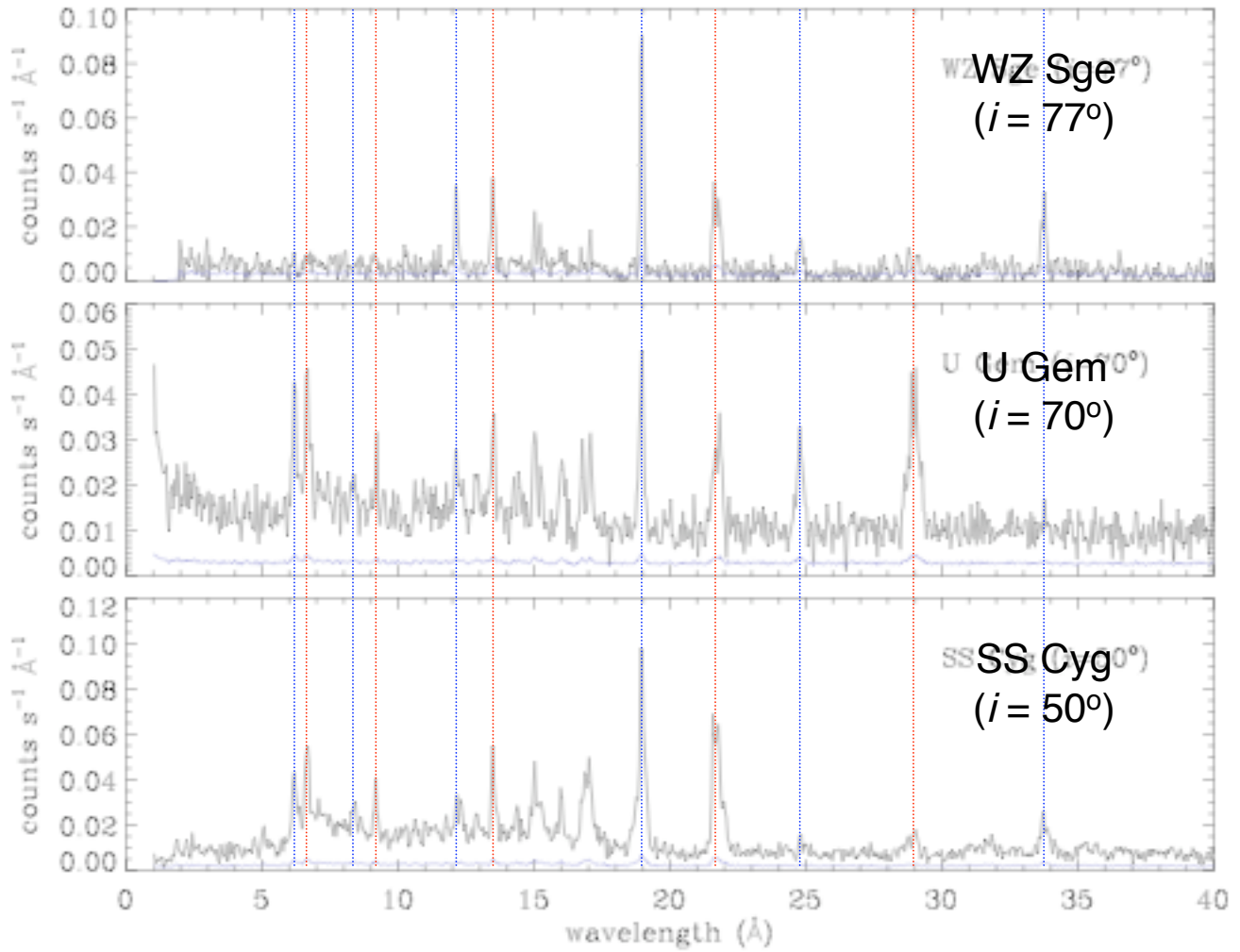
EUVE SW and Chandra LETG spectra of dwarf novae in outburst



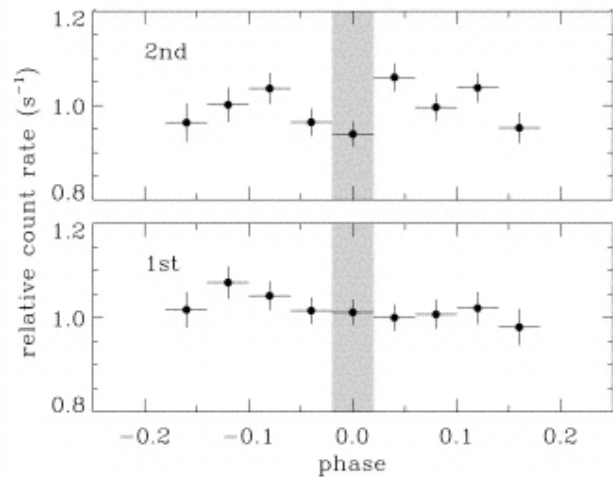
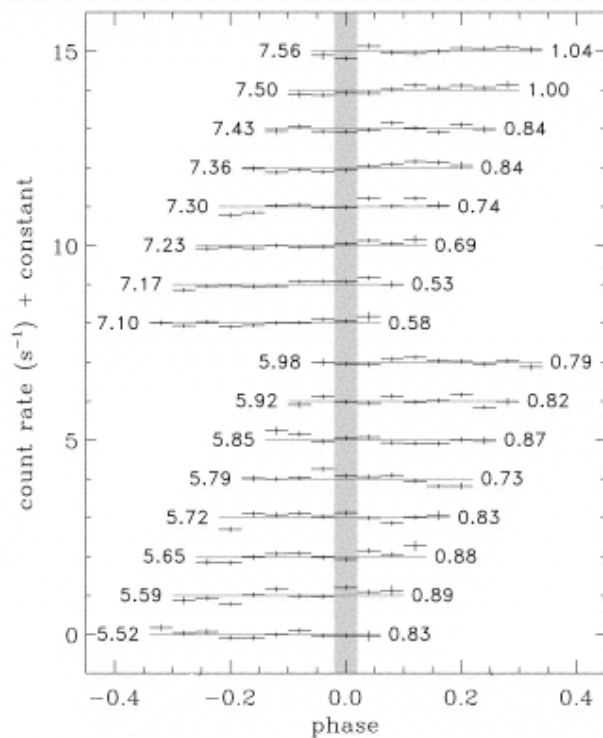
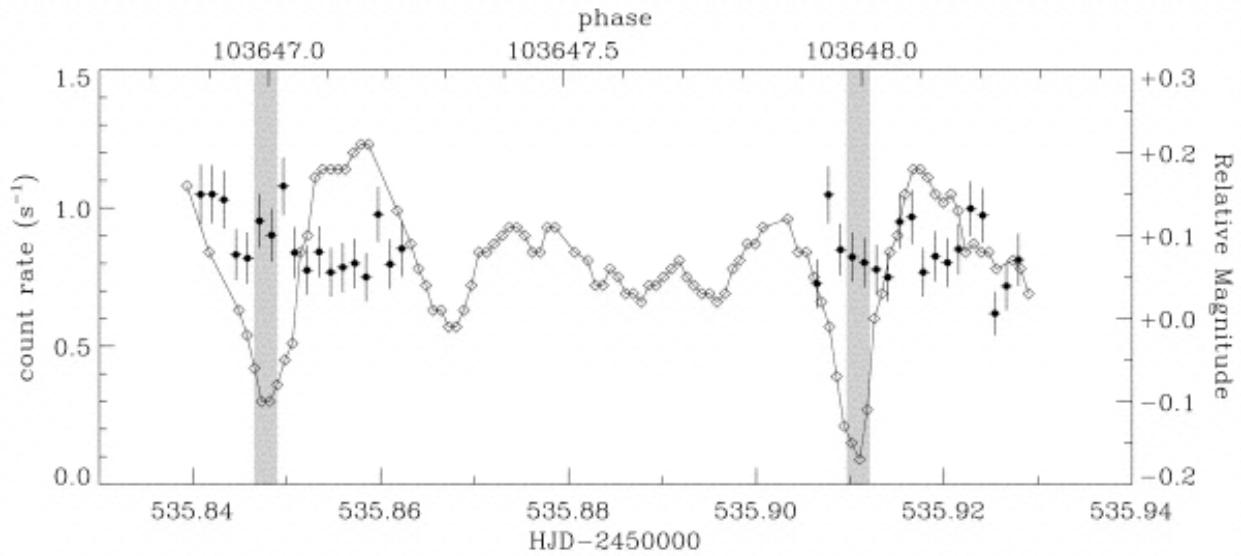
EUVE SW and Chandra LETG spectra of dwarf novae in outburst



Chandra LETG spectra of dwarf novae in outburst



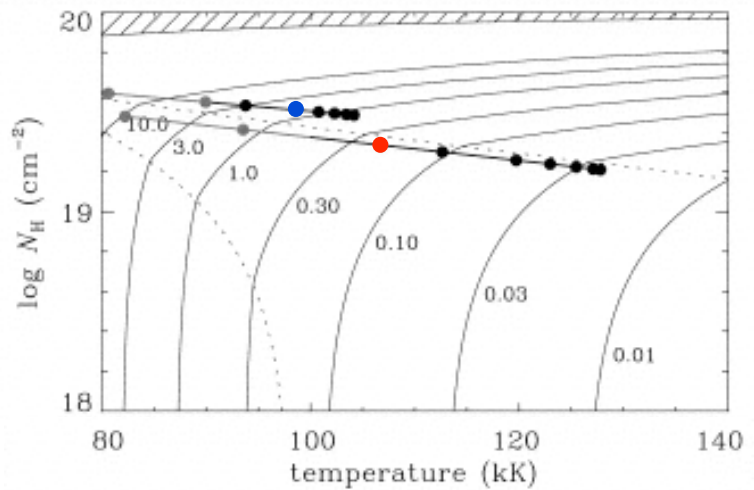
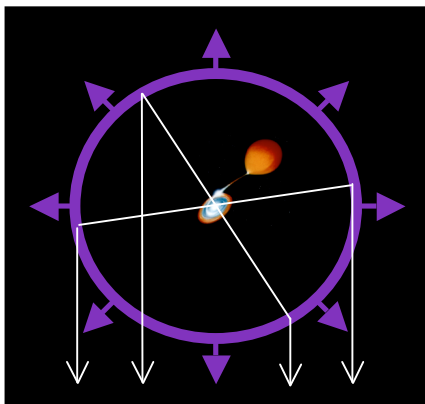
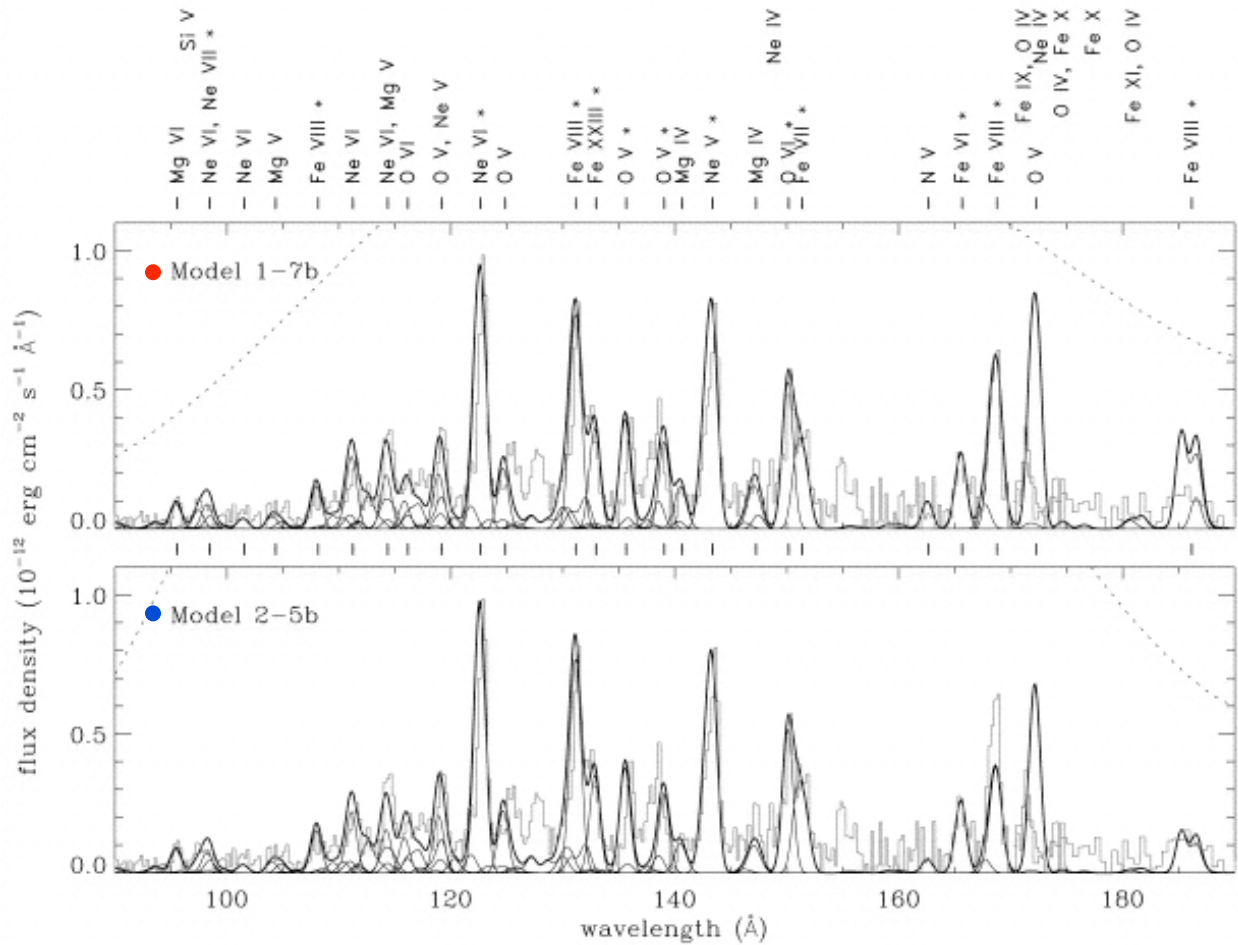
Optical & EUVE DS light curves of OY Car



EUUV flux is not eclipsed by the white dwarf

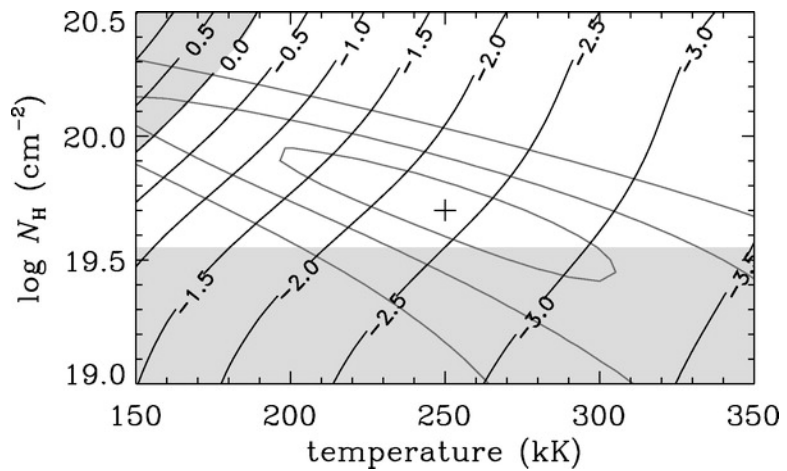
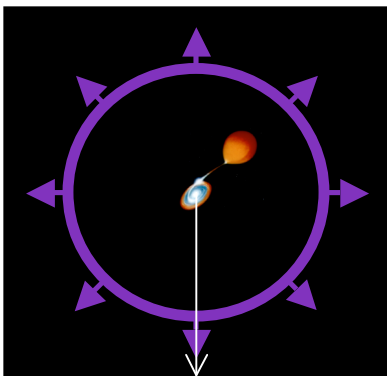
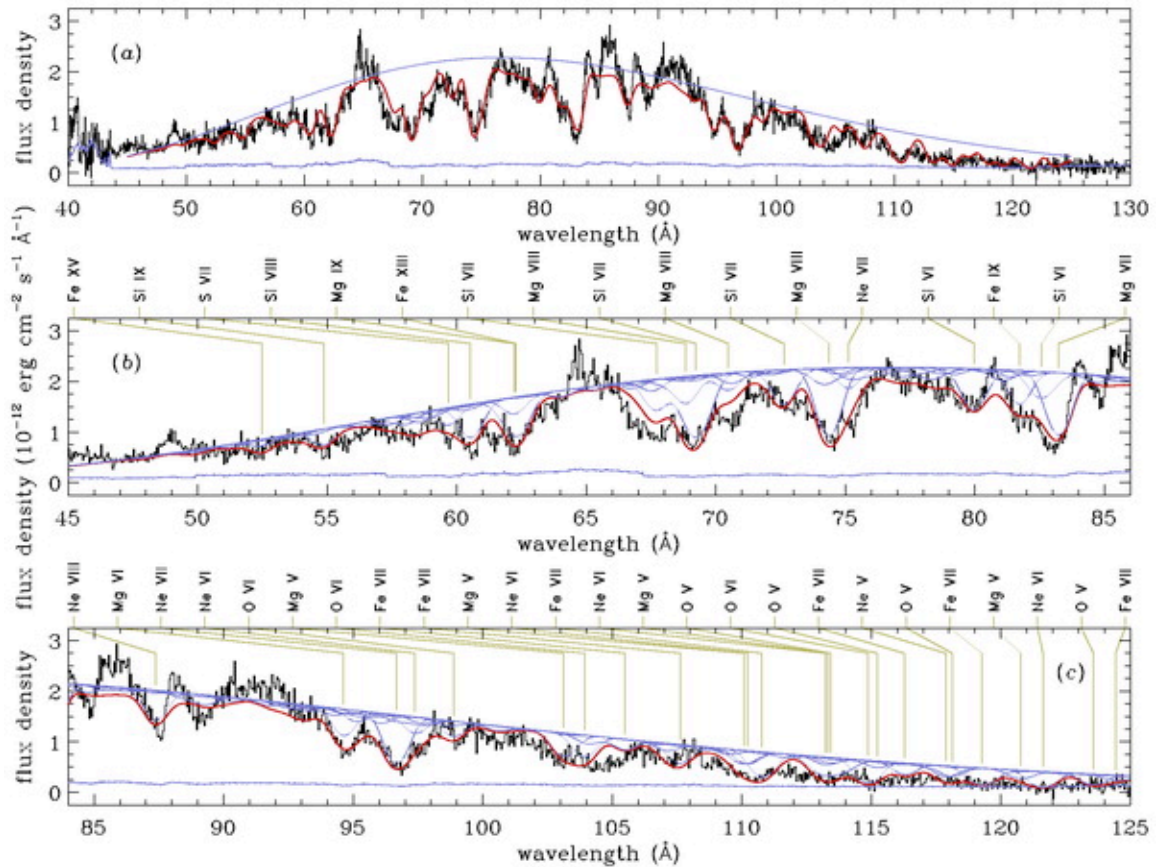
Mauche & Raymond (2000, ApJ, 541, 924)

Model of the *EUVE* SW spectrum of OY Car



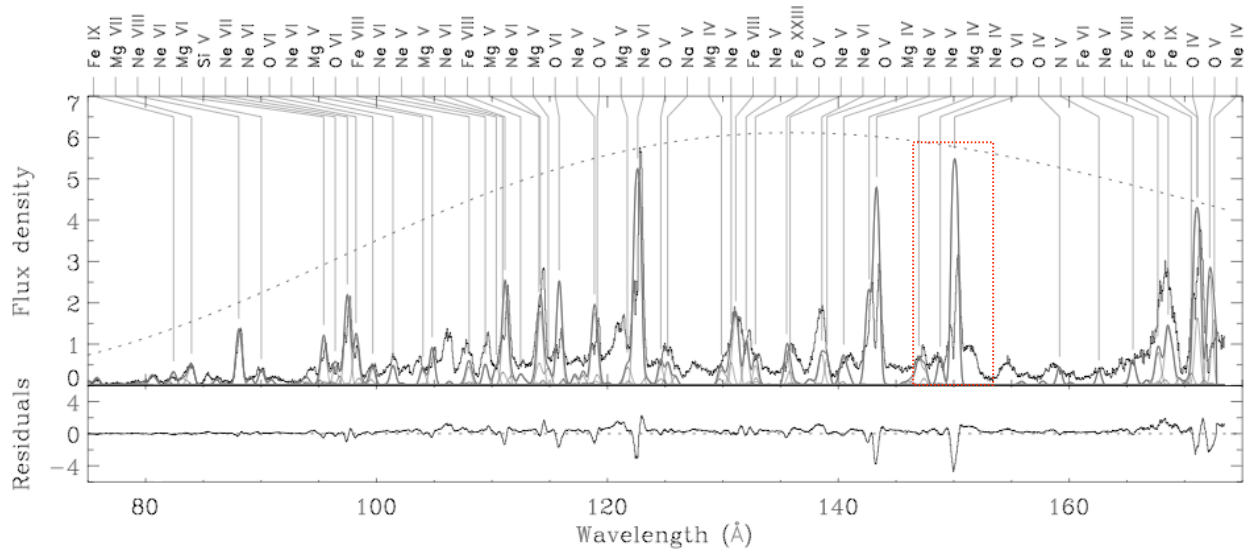
Mauche & Raymond (2000, ApJ, 541, 924)

Model of the *Chandra* LETG spectrum of SS Cyg

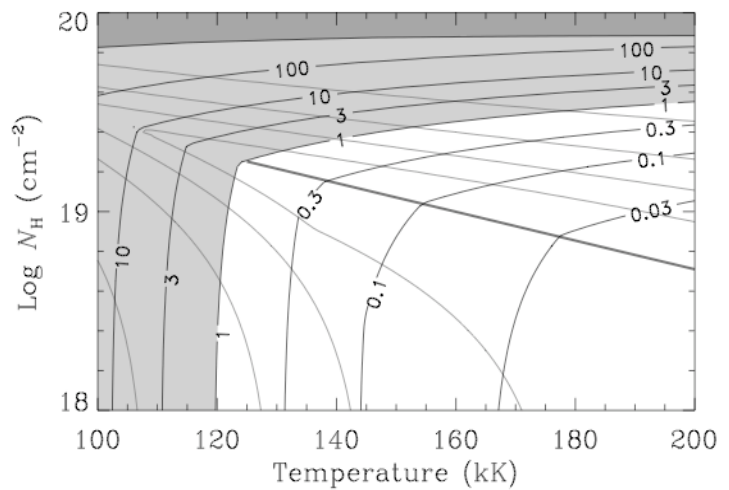
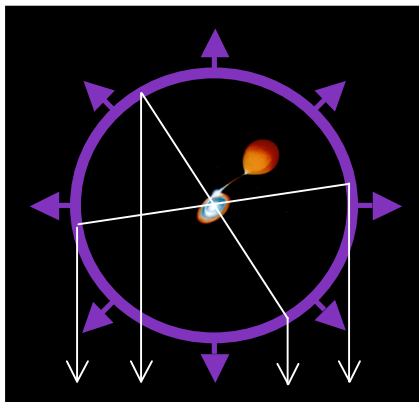
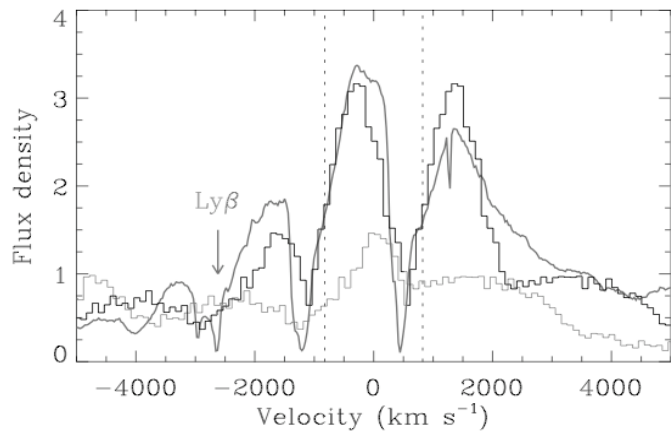


Mauche (2004, ApJ, 610, 422)

Chandra LETG spectrum of WZ Sge

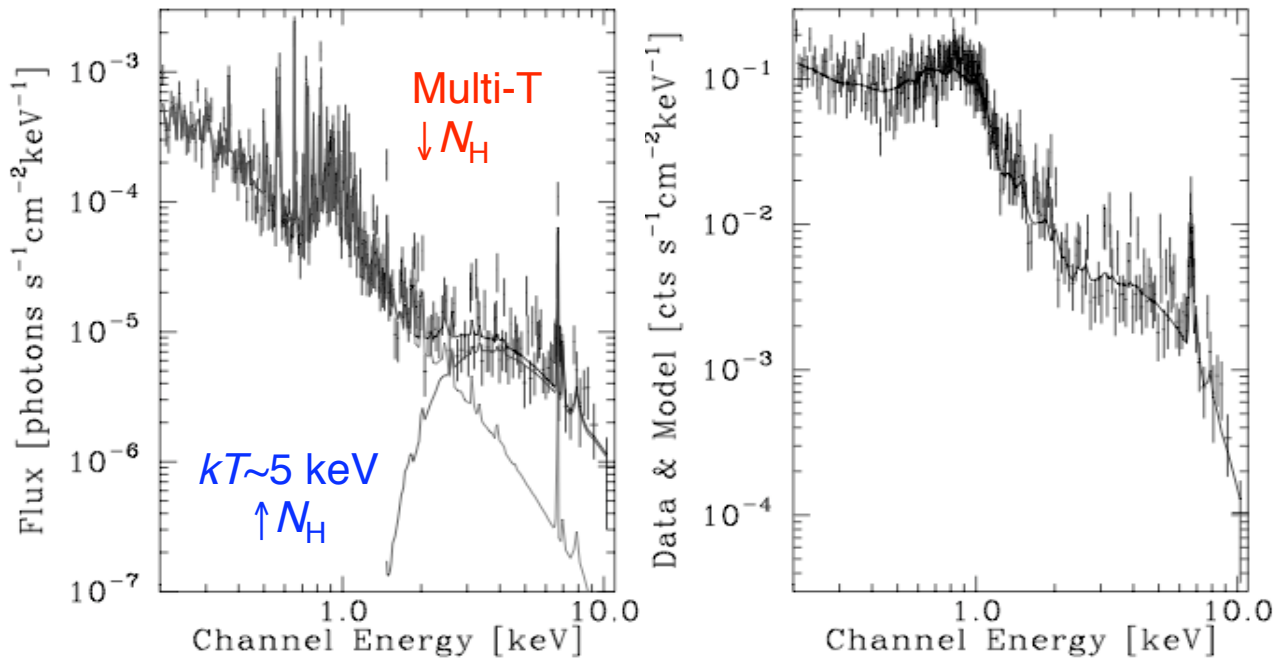
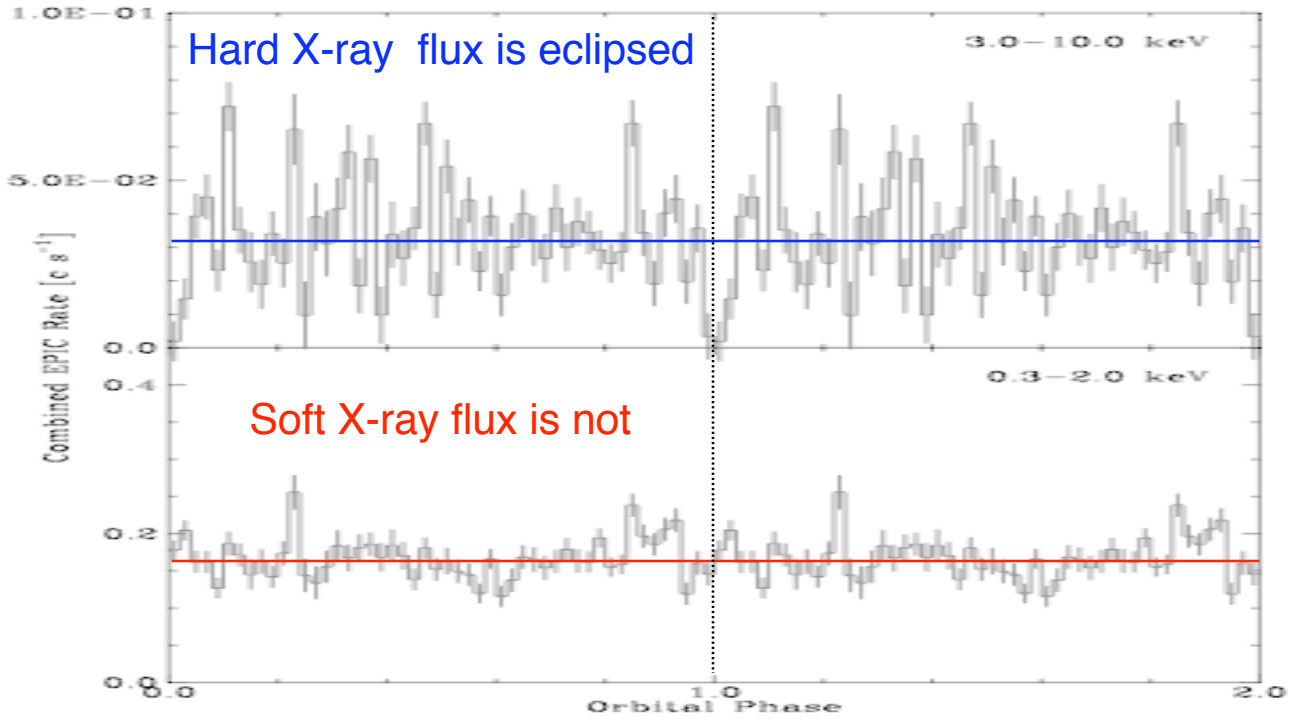


O VI 2s-2p
 $\lambda 150$ (*Chandra*)
 $\lambda 1032, 1038$ (*FUSE*)



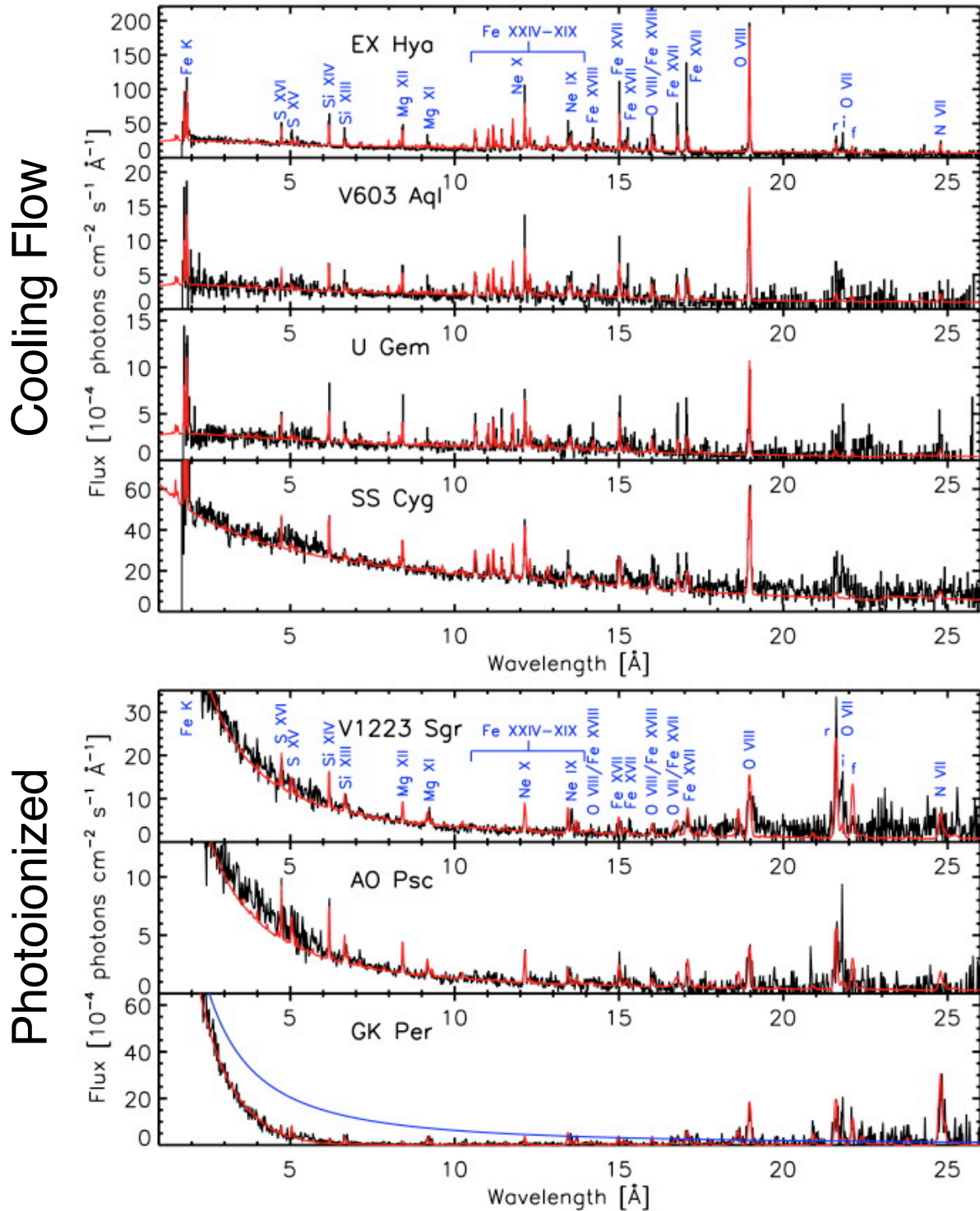
Wheatley & Mauche (2007, in preparation)

XMM EPIC light curves and spectra show two sources of X-ray emission in UX UMa



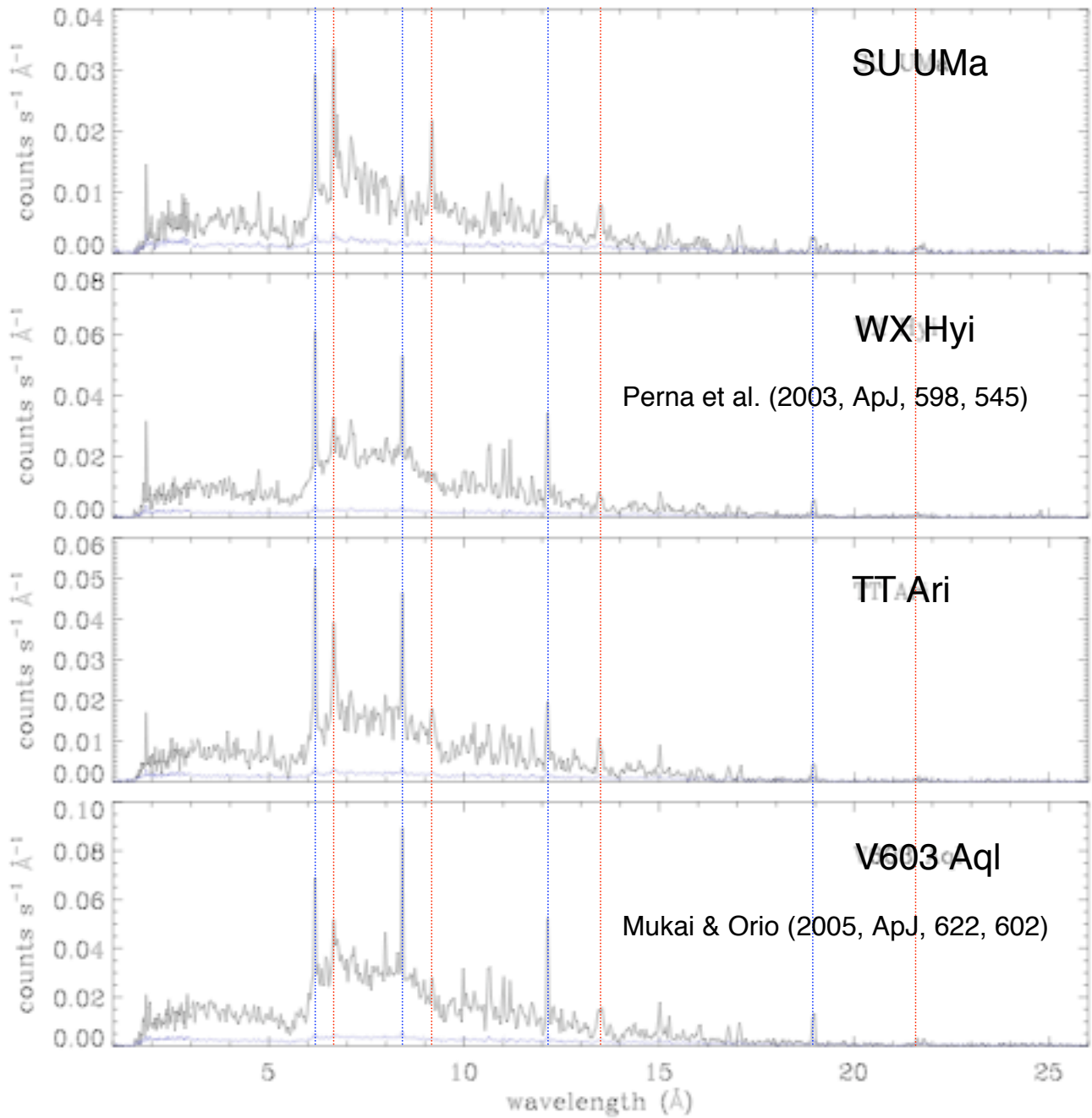
Pratt et al. (2004, MNRAS, 348, L49)

Two types of X-ray spectra in CVs

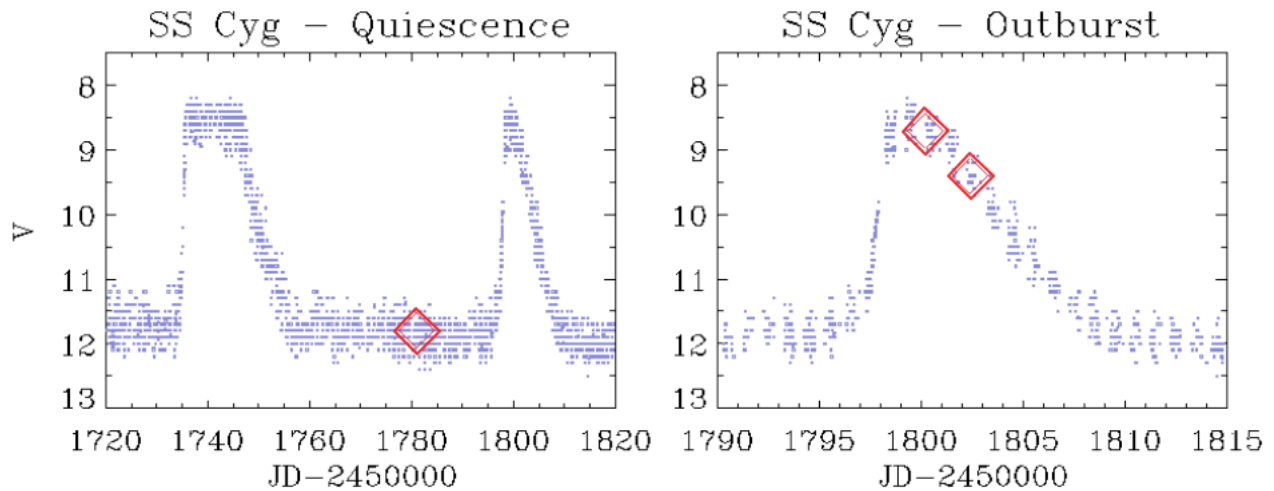


Mukai et al. (2003, ApJ, 586, 77)

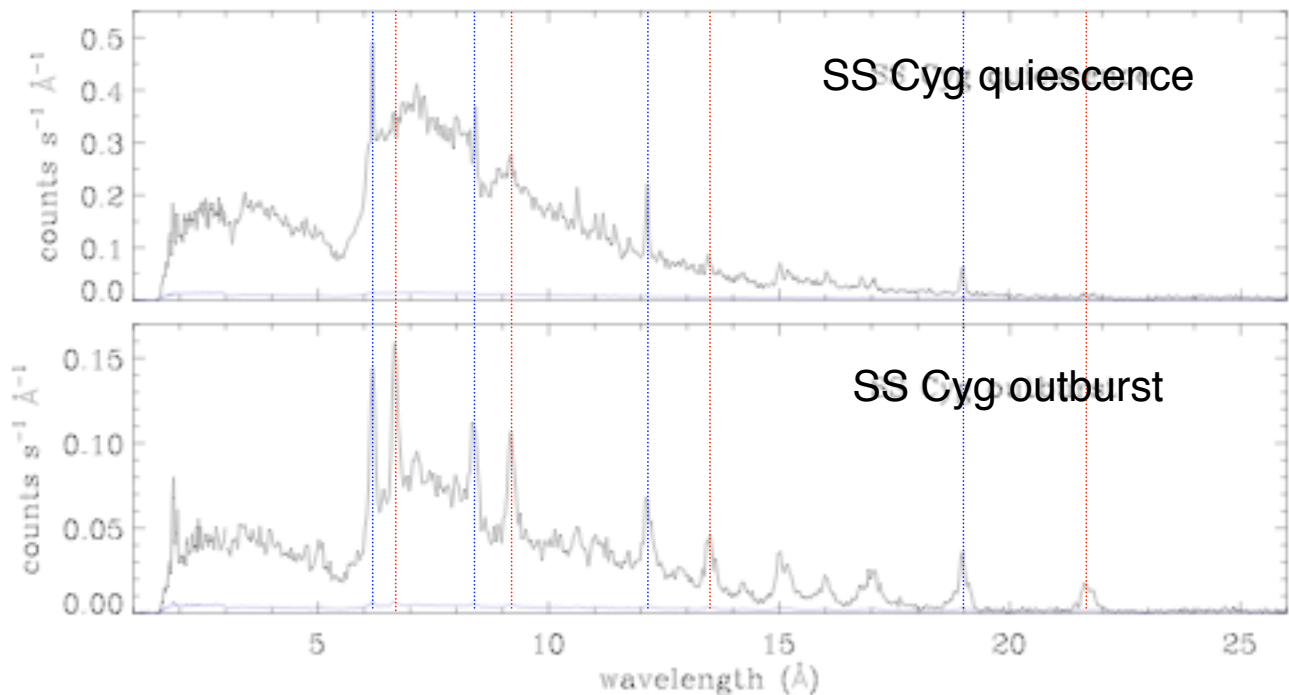
Chandra HETG spectra of nonmagnetic CVs



Chandra HETG spectra of SS Cyg in quiescence and outburst

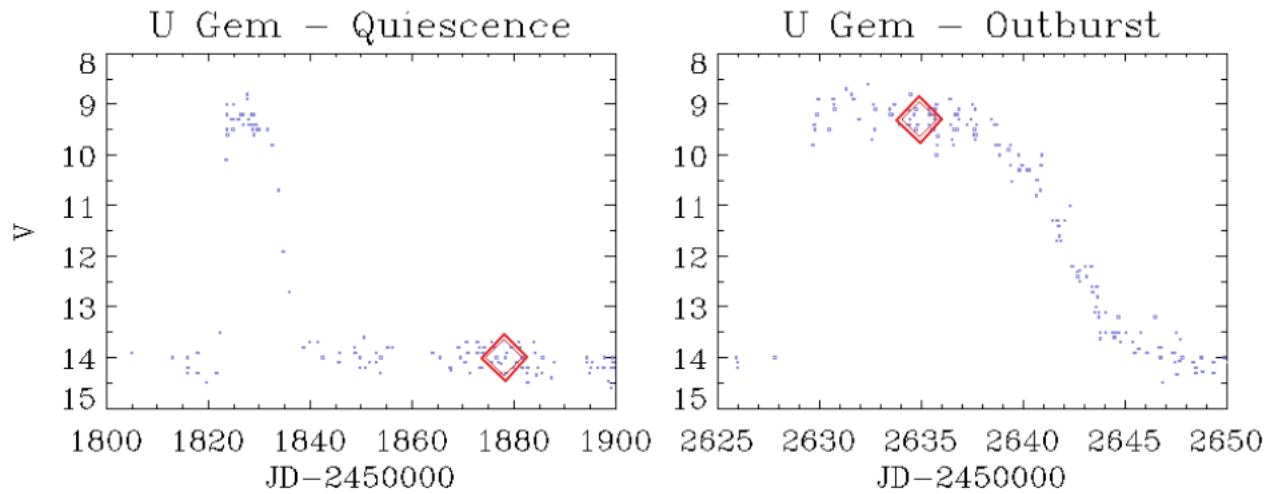


X-ray flux *decreases* in outburst, lines broaden.

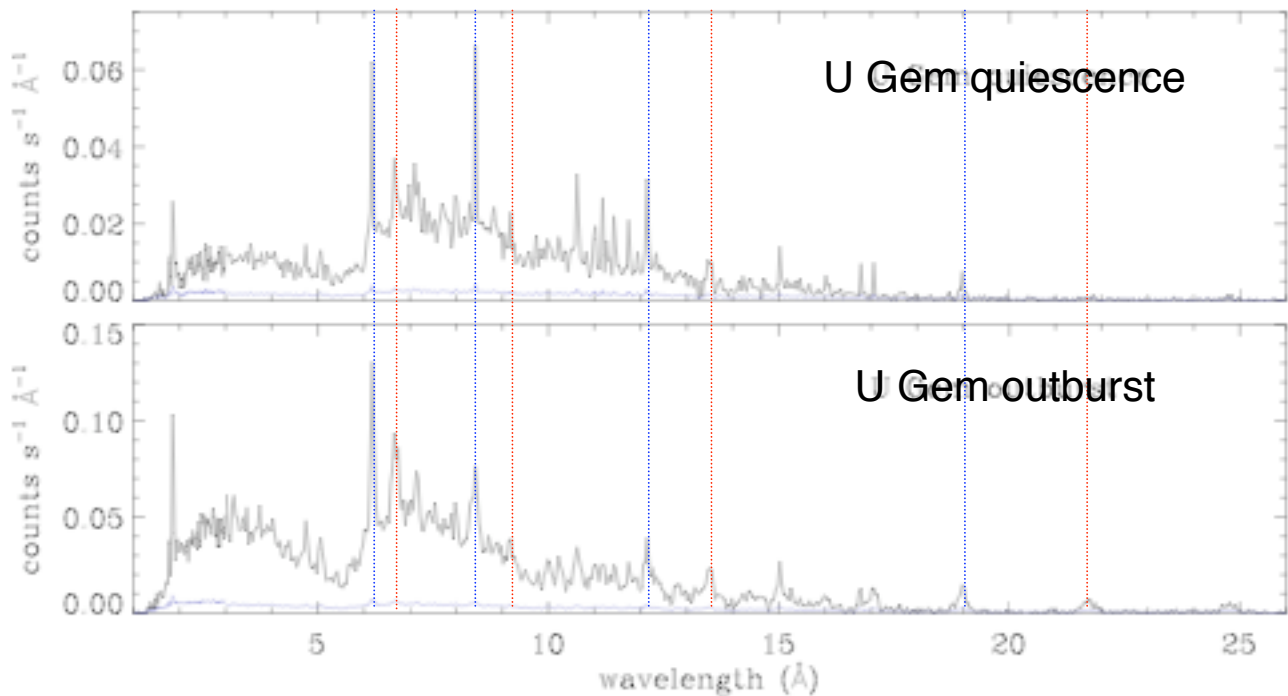


Mauche et al. (2005, in Astrophysics of CVs & Related Objects)

Chandra HETG spectra of U Gem in quiescence and outburst



X-ray flux *increases* in outburst, lines broaden.

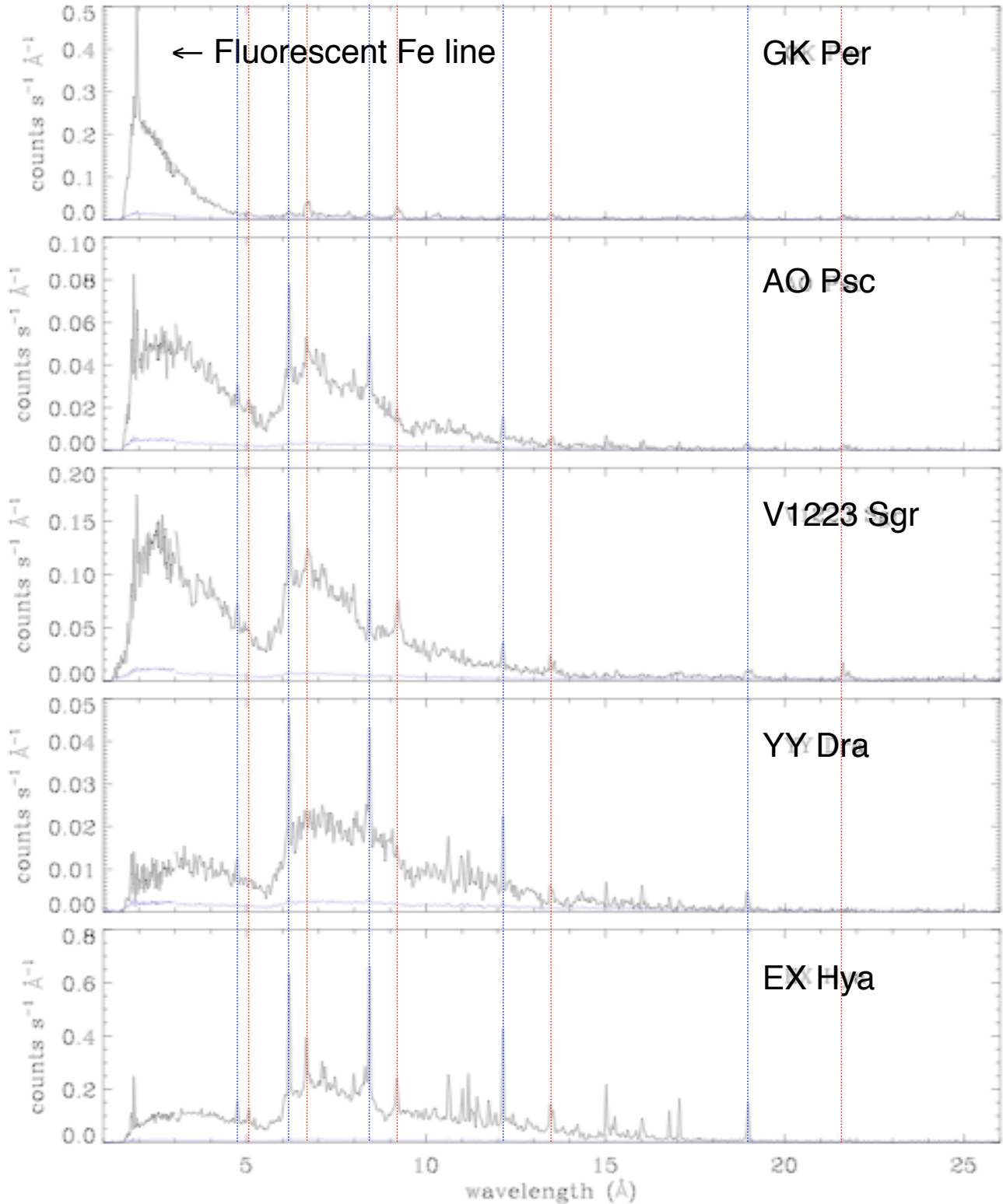


Szkody et al. (2002, ApJ, 574, 942)

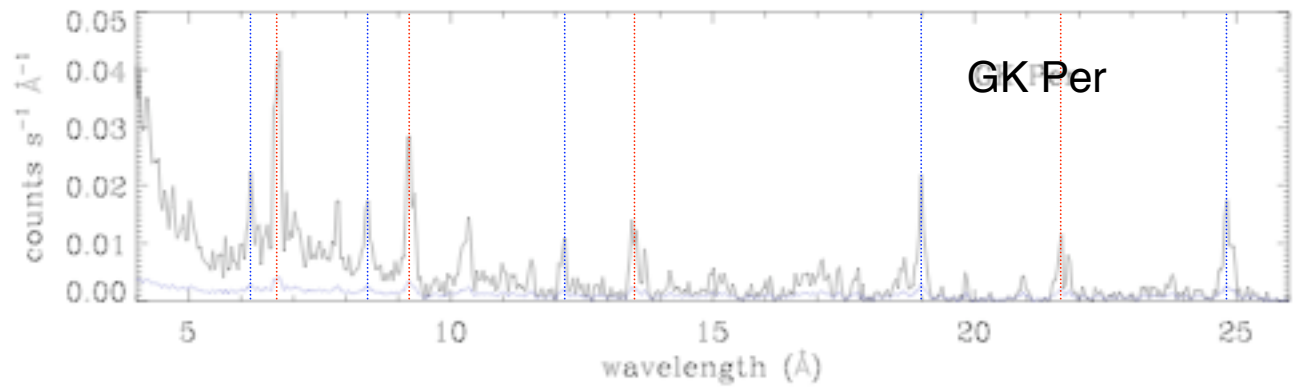
Mauche et al. (2005, in Astrophysics of CVs & Related Objects)

Güver et al. (2006, MNRAS, 372, 450)

Chandra HETG spectra of IPs



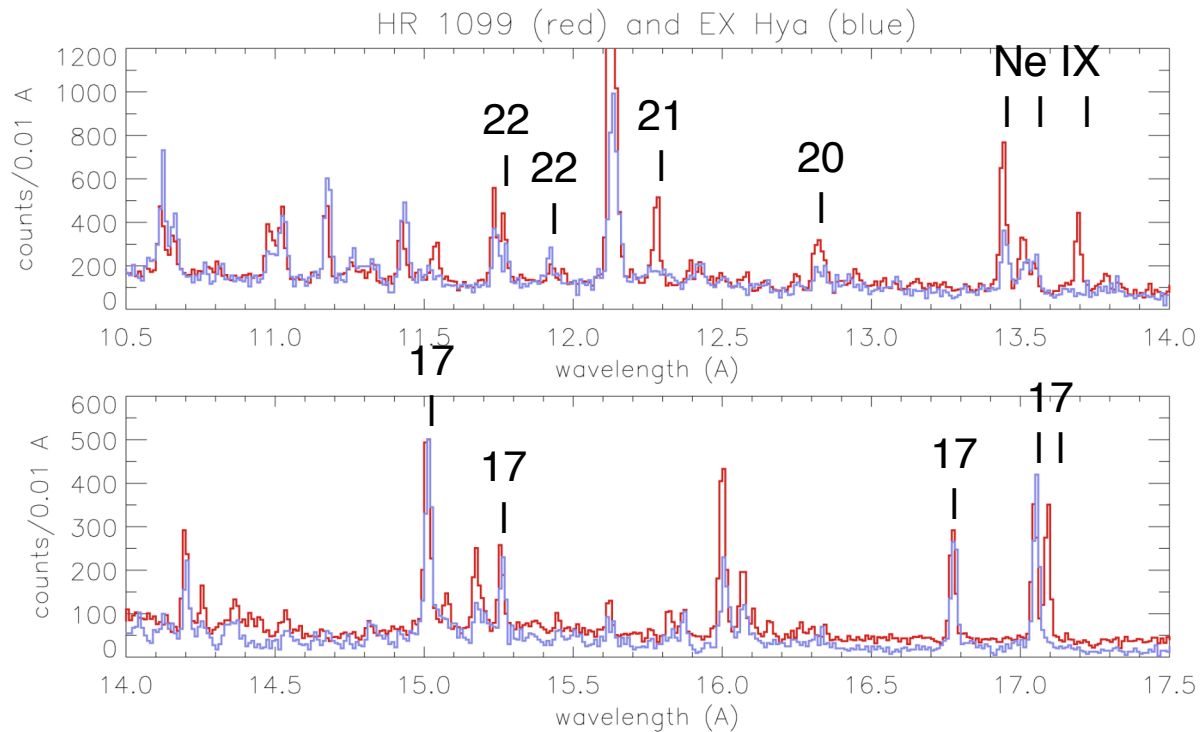
Detail of *Chandra* HETG spectrum of GK Per



Al XI ?-

Ne IX RRC ?-

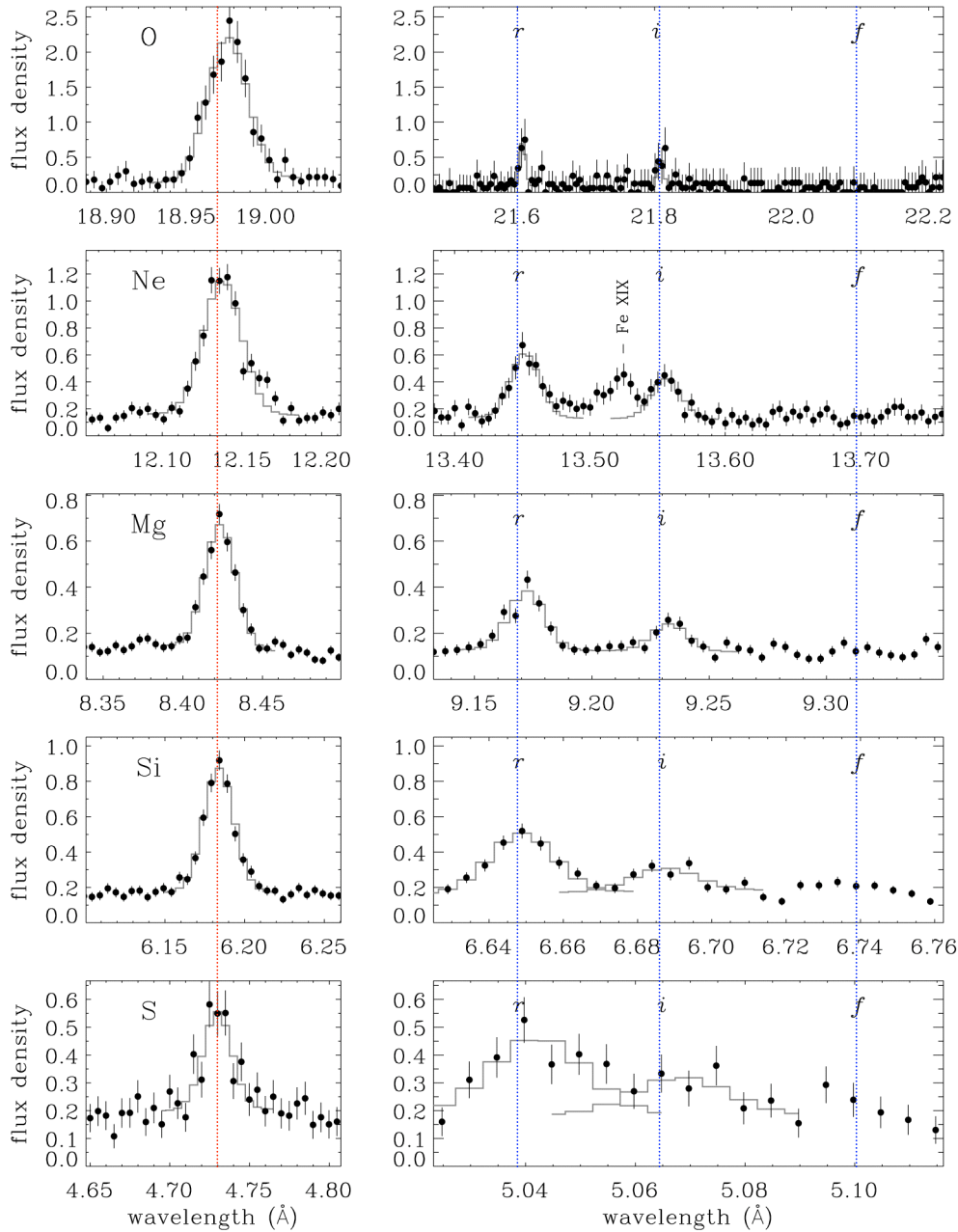
Comparison of HR 1099 and EX Hya



EX Hya is missing lines of: Fe XVII λ 17.10, Fe XX λ 12.80, Fe XXI λ 12.26, and has an inverted Fe XXII λ 11.92/ λ 11.77 ratio.

Mauche, Liedahl, & Fournier (2005, in X-ray Diagnostics of Astrophysical Plasmas: Theory, Experiment, & Observation)

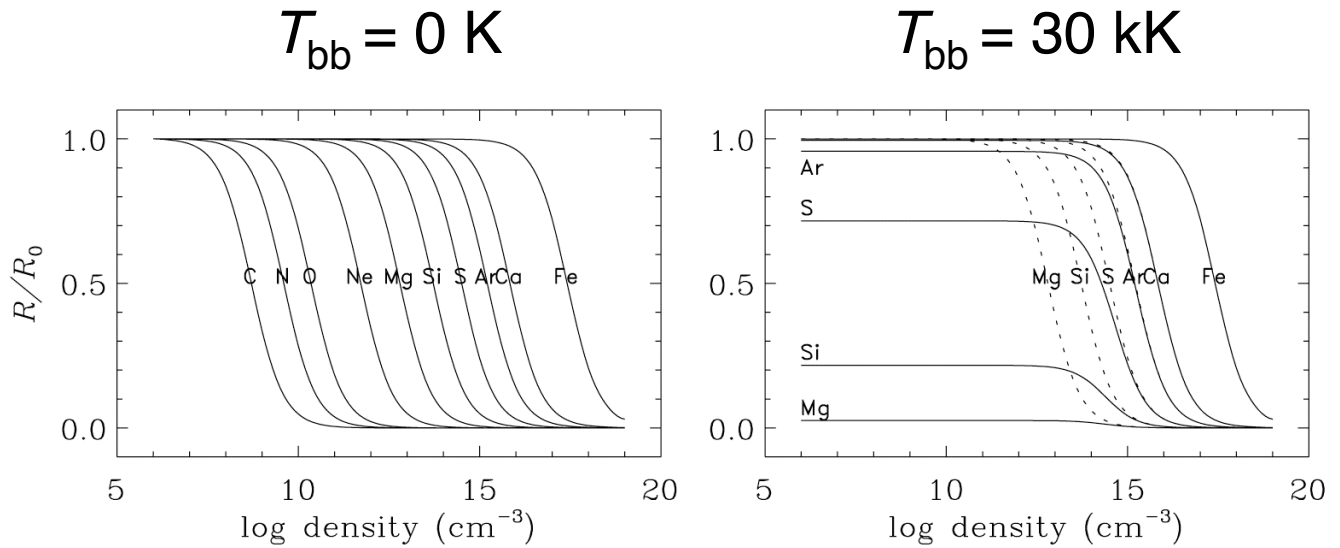
H- and He-like lines of EX Hya



All the He-like *f* lines are missing in EX Hya.

Mauche (2002, in Physics of CVs and Related Objects)

He-like $R = z/(x+y) = f/i$ line ratios



Absence of He-like f lines in EX Hya is plausibly due to photoexcitation.

Mauche (2002, in Physics of CVs and Related Objects)

Theoretical Fe L-shell spectra



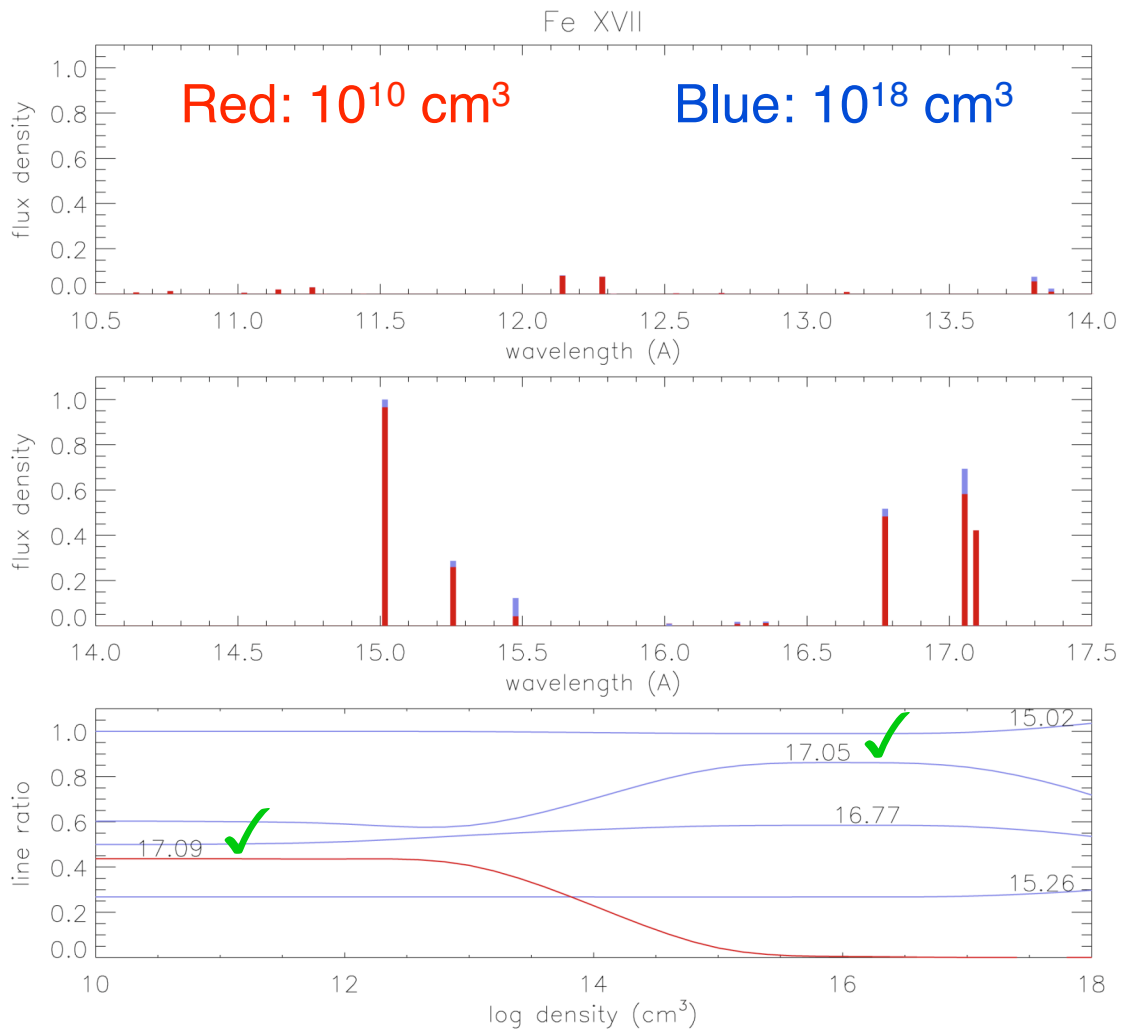
...were calculated with the Livermore X-ray Spectral Synthesizer (LXSS), a suite of IDL codes that calculates spectral models as a function of temperature and electron density using primarily HULLAC atomic data.

The following spectra are based on models with:

Ion	levels	radrate	colrate
Fe XXIV	76	4,100	1,704
Fe XXIII	116	8,798	6,478
Fe XXII	228	37,300	24,084
Fe XXI	591	227,743	153,953
Fe XX	609	257,765	165,350
Fe XIX	605	240,948	164,496
Fe XVIII	456	141,229	93,583
Fe XVII	281	49,882	33,887

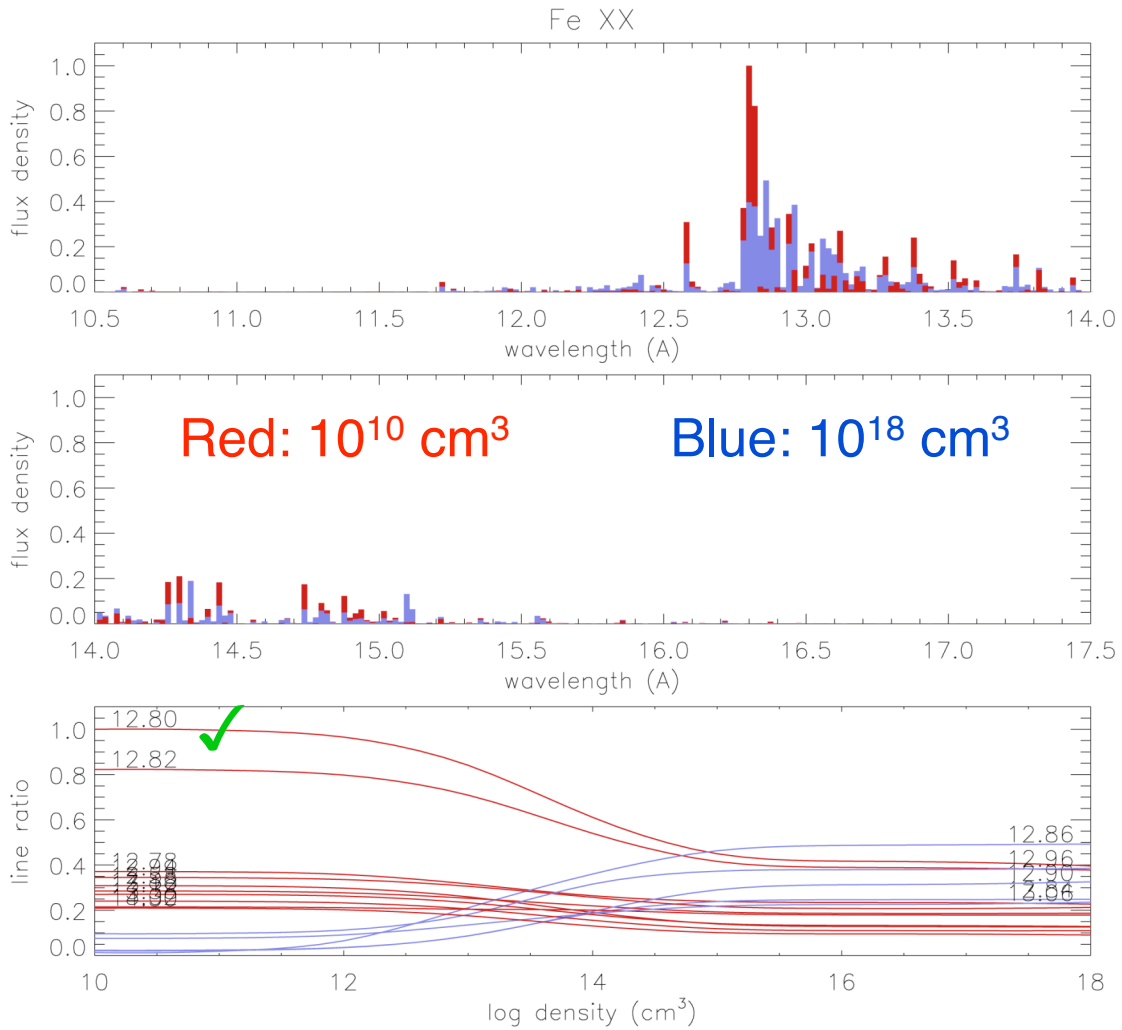
Mauche, Liedahl, & Fournier (2005, in X-ray Diagnostics of Astrophysical Plasmas: Theory, Experiment, & Observation)

Fe XVII



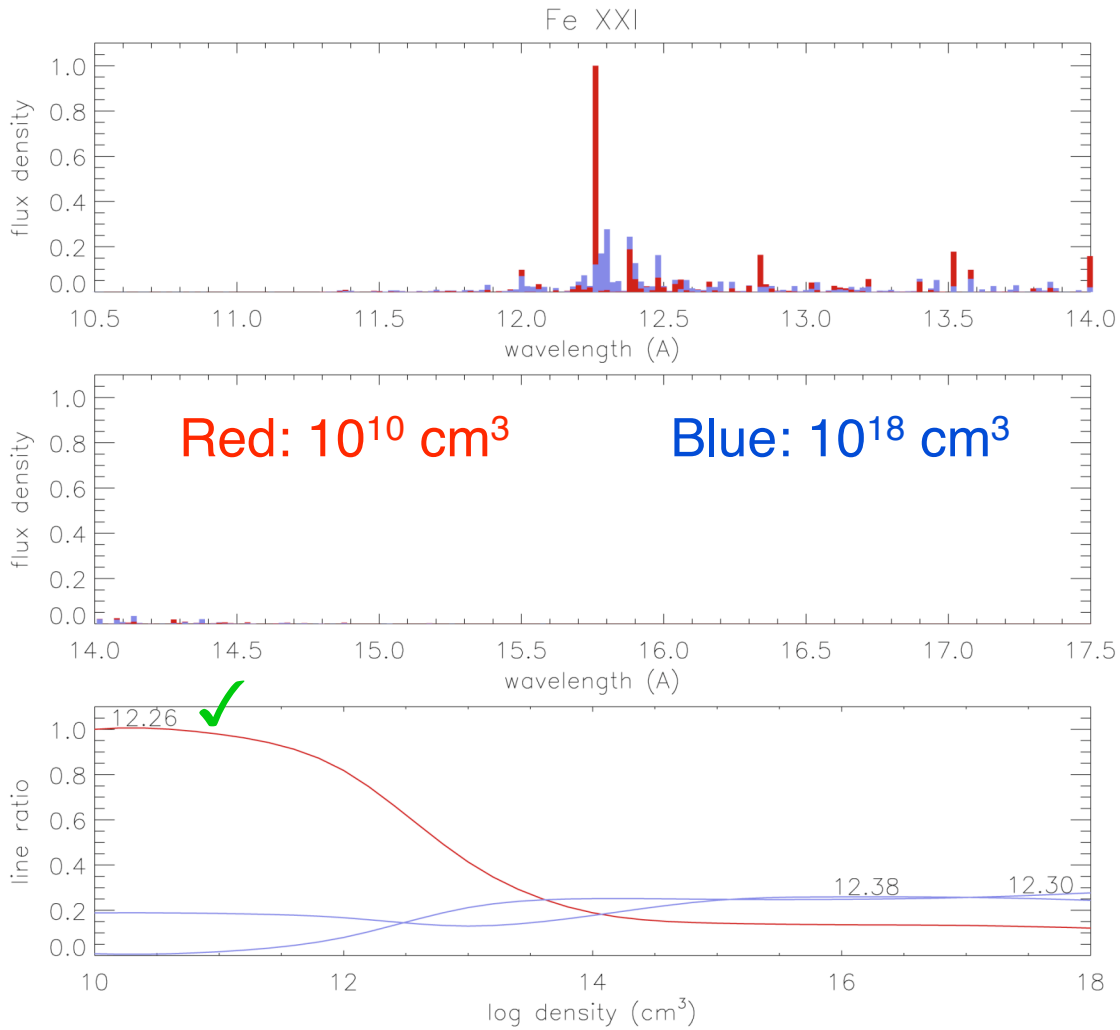
Mauche, Liedahl, & Fournier (2005, in X-ray Diagnostics of Astrophysical Plasmas: Theory, Experiment, & Observation)

Fe XX



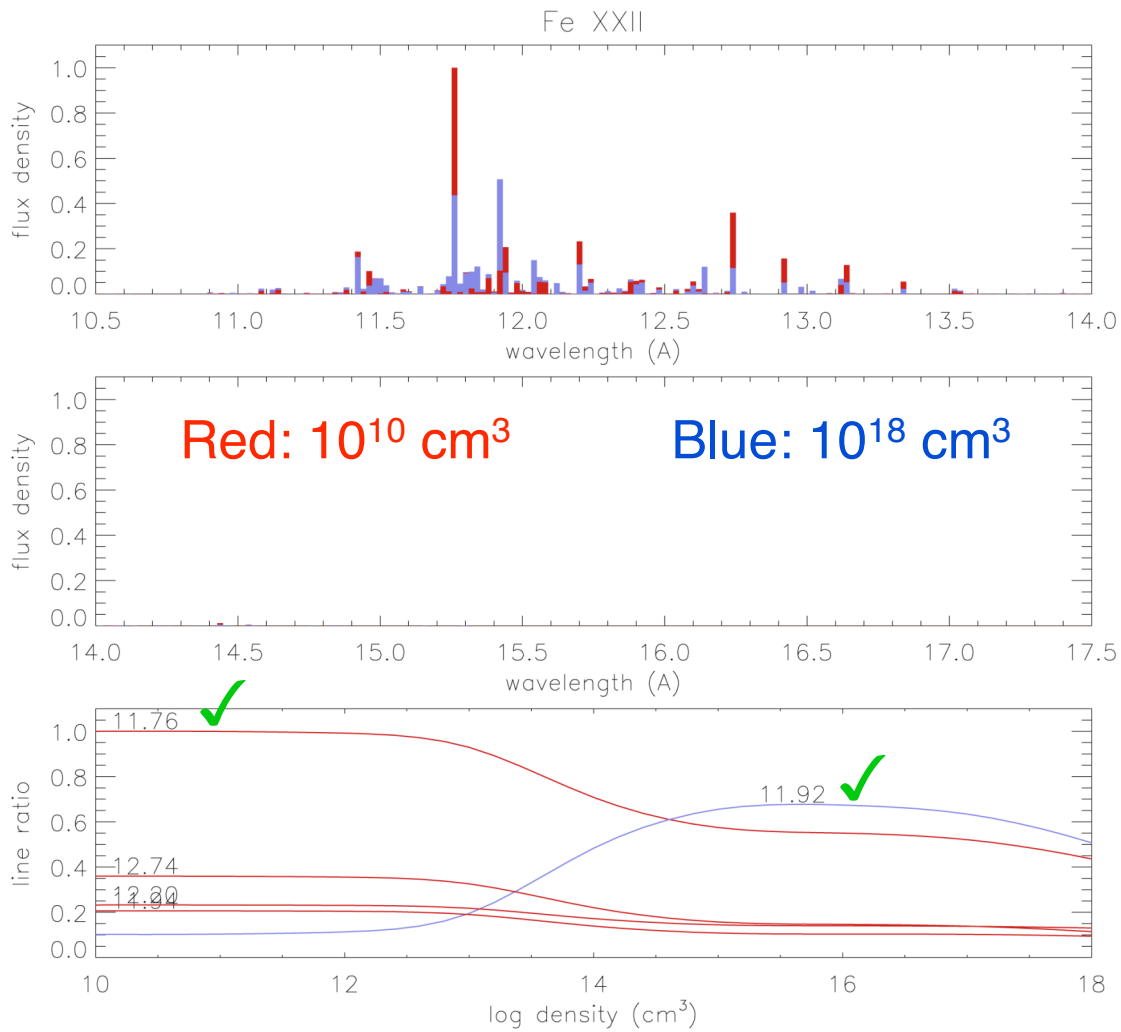
Mauche, Liedahl, & Fournier (2005, in X-ray Diagnostics of Astrophysical Plasmas: Theory, Experiment, & Observation)

Fe XXI



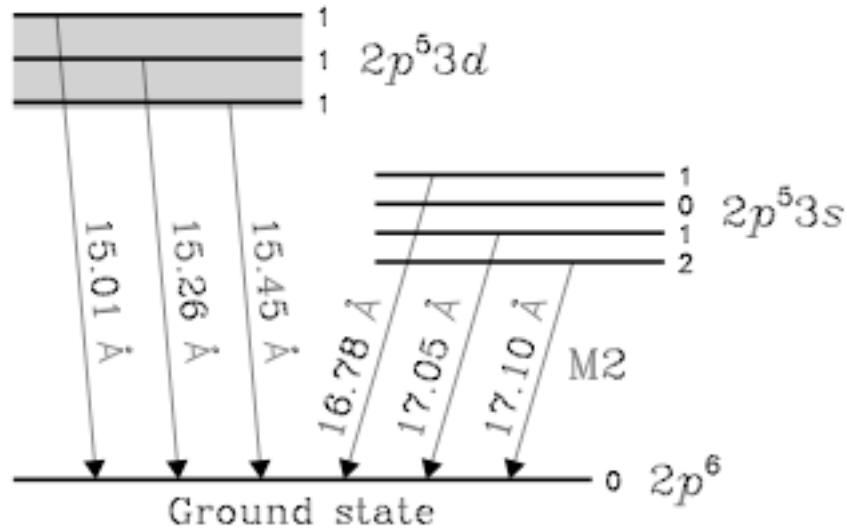
Mauche, Liedahl, & Fournier (2005, in X-ray Diagnostics of Astrophysical Plasmas: Theory, Experiment, & Observation)

Fe XXII

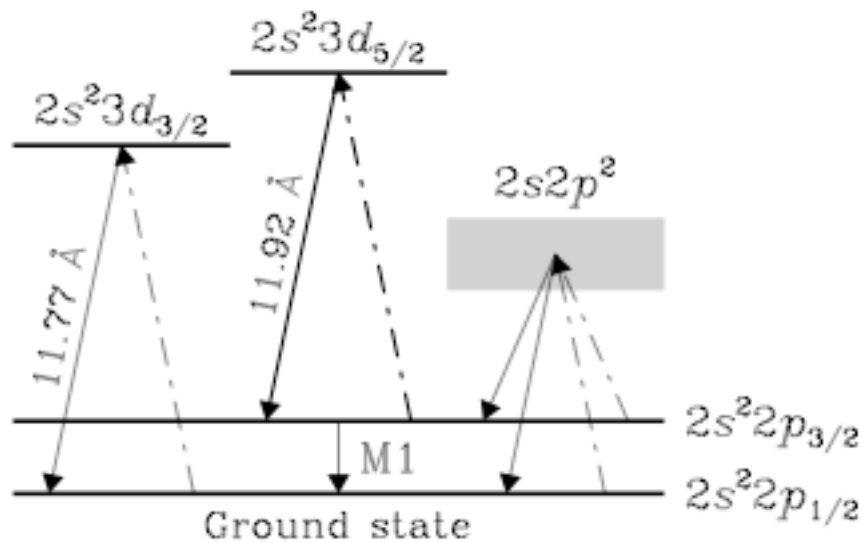


Mauche, Liedahl, & Fournier (2005, in X-ray Diagnostics of Astrophysical Plasmas: Theory, Experiment, & Observation)

Grotrian diagrams for Fe XVII and Fe XXII



Fe XVII

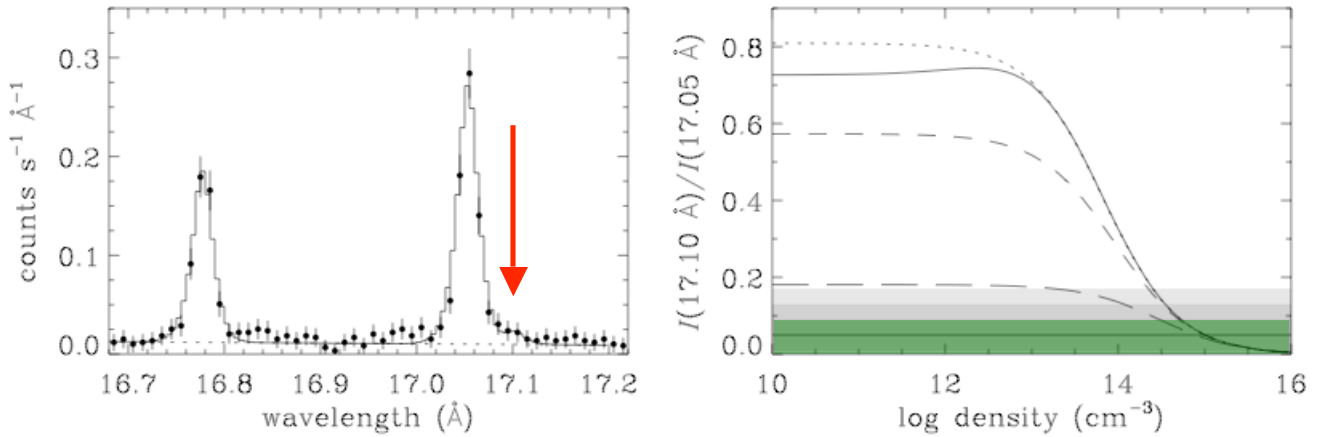


Fe XXII

Mauche, Liedahl, & Fournier (2005, in X-ray Diagnostics of Astrophysical Plasmas: Theory, Experiment, & Observation)

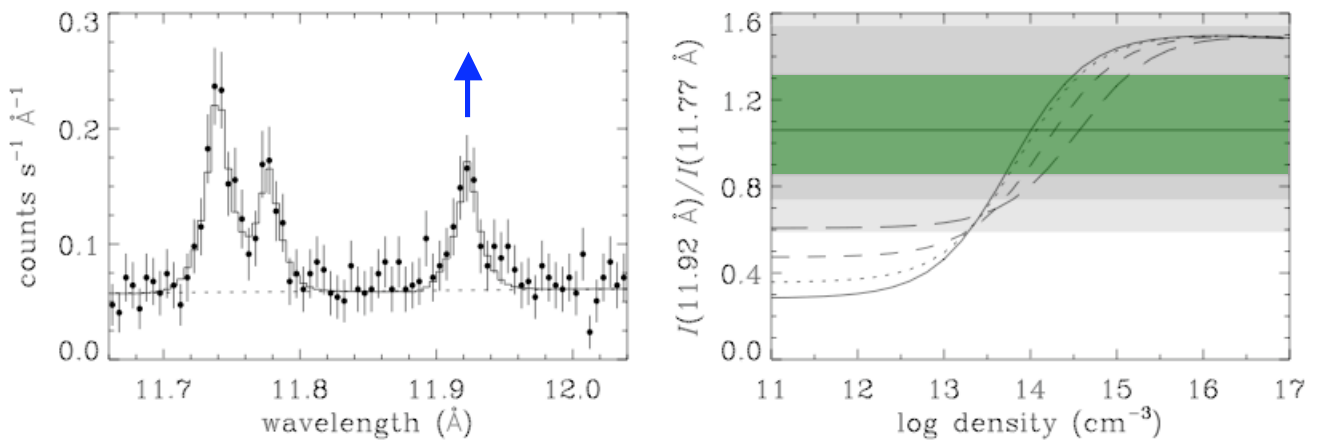
Density constraints from Fe XVII $\lambda 17.10 / \lambda 17.05$ and Fe XXII $\lambda 11.92 / \lambda 11.77$

Fe XVI: $n_e > 2 \times 10^{14} \text{ cm}^{-3}$



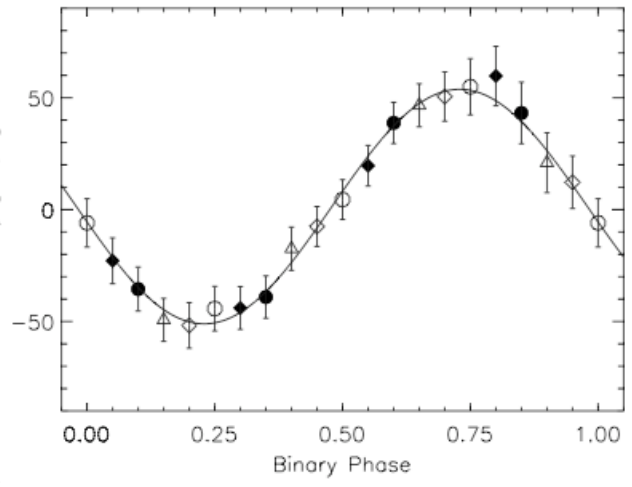
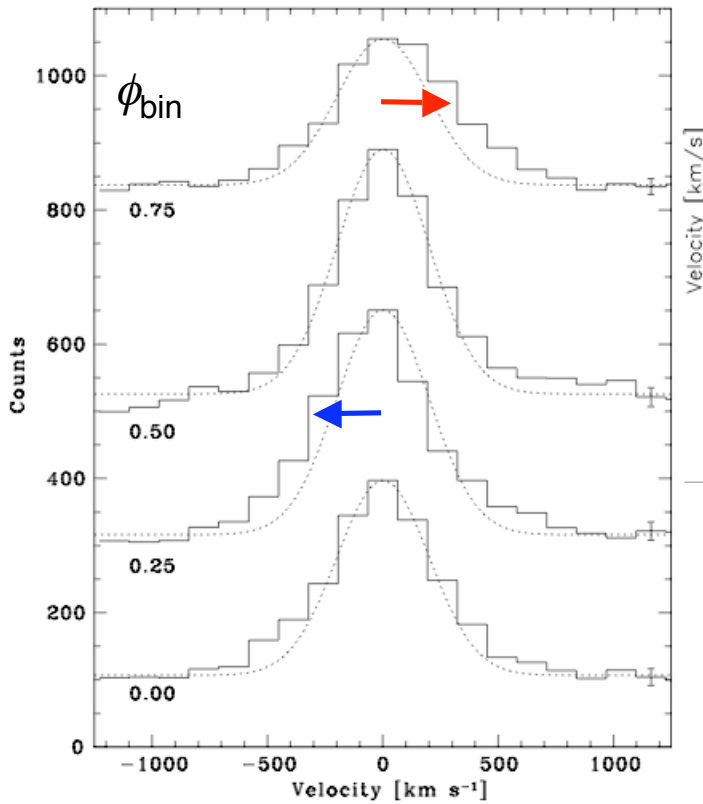
Mauche, Liedahl, & Fournier (2001, ApJ, 560, 992)

Fe XXII: $n_e \sim 1 \times 10^{14} \text{ cm}^{-3}$



Mauche, Liedahl, & Fournier (2003, ApJ, 588, L101)

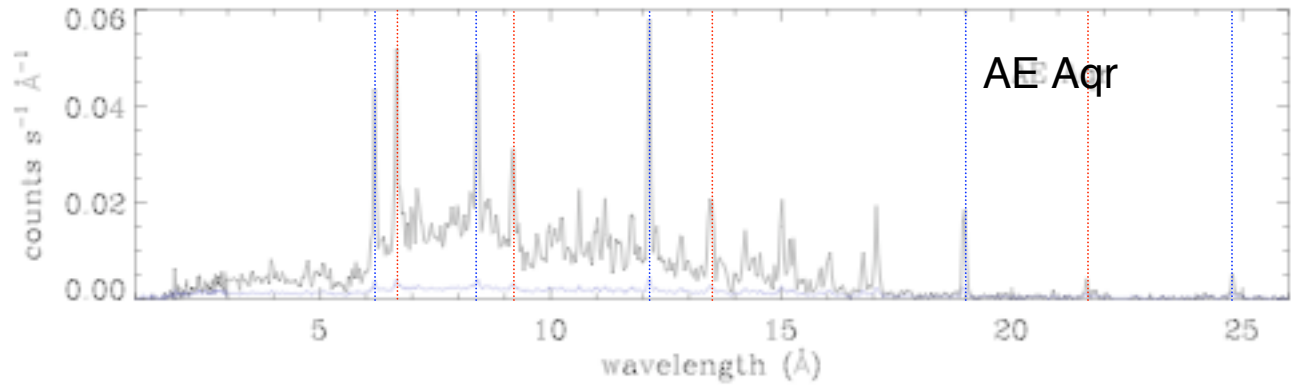
Radial velocity variations of the X-ray emission lines of EX Hya



$$\begin{aligned} \gamma &= 1.3 \pm 2.3 \text{ km s}^{-1} \\ K &= 58.2 \pm 3.7 \text{ km s}^{-1} \\ M_{\text{wd}} &= 0.49 \pm 0.13 M_{\odot} \end{aligned}$$

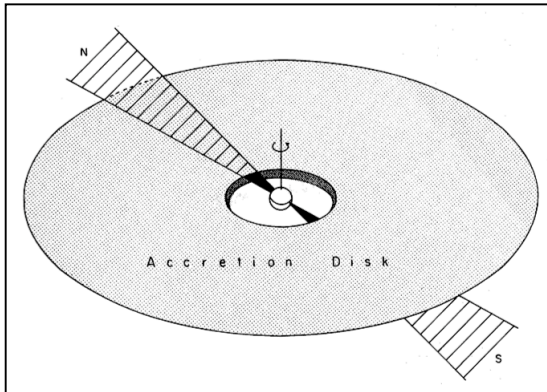
Dynamically-derived white dwarf mass agrees with the value obtained from the Fe XXV/XXVI line ratio in the *ASCA* SIS spectrum of EX Hya (Fujimoto & Ishida 1997).

Chandra HETG spectrum of AE Aqr (an IP with $P_{\text{binary}} = 9.88$ hr, $P_{\text{spin}} = 33.08$ s, $i \approx 60^\circ$)



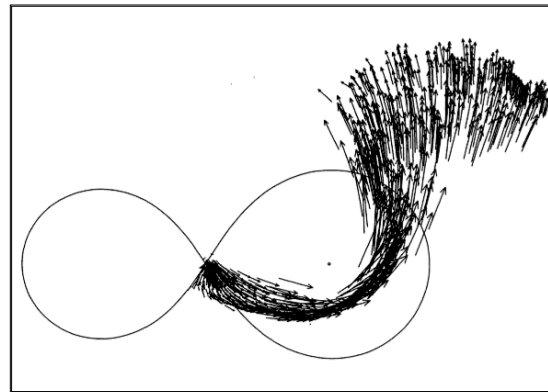
Different physical models for AE Aqr:

Oblique rotator model



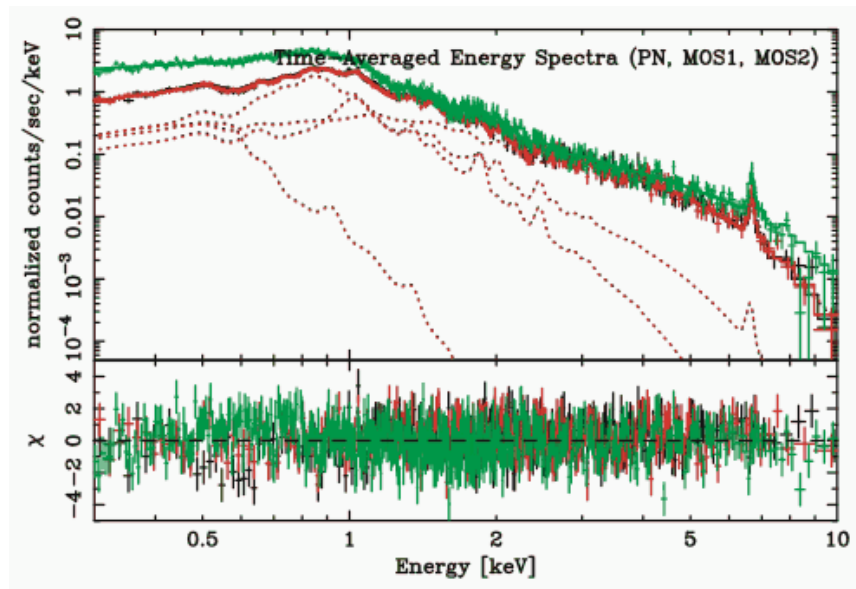
Patterson (1979)

Magnetic propeller model

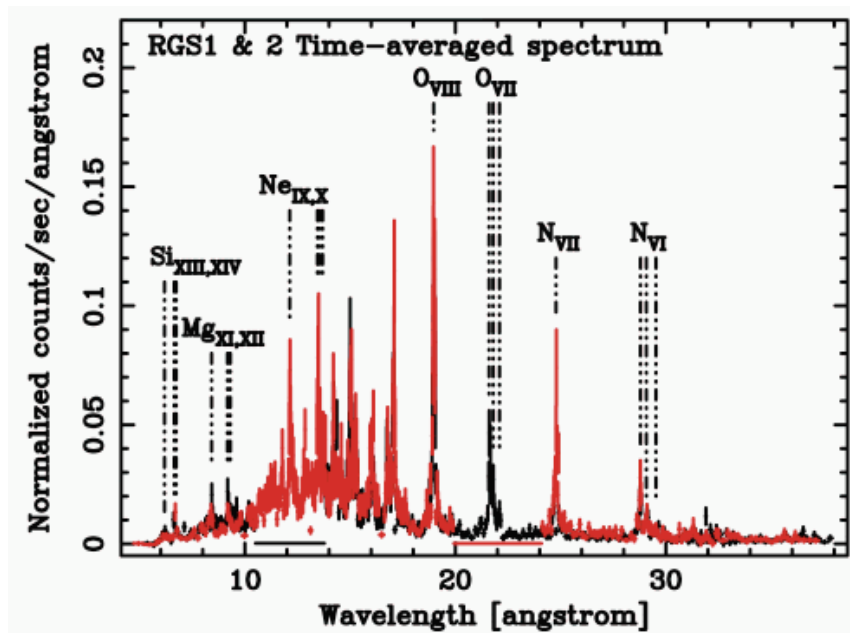


Wynn, King, & Horne (1997)

XMM EPIC & RGS spectra of AE Aqr

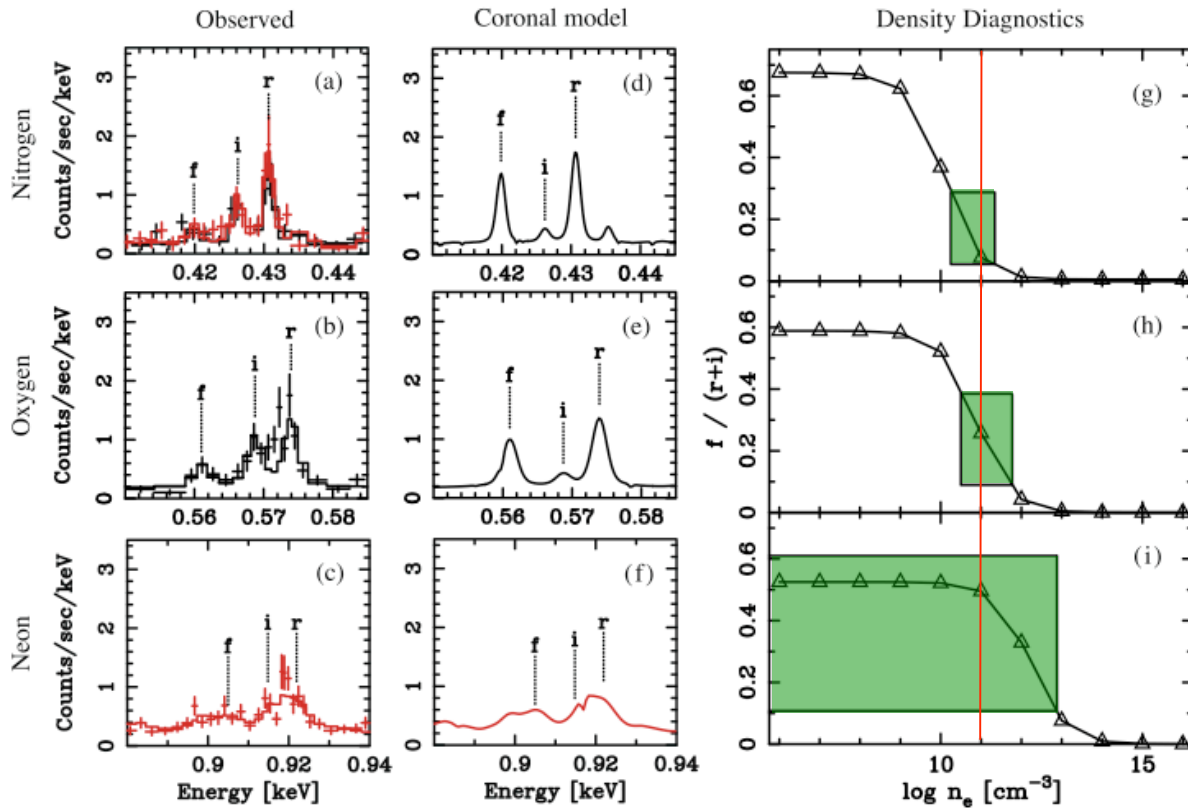


4T VMEKAL:
 $kT = 0.14, 0.59, 1.21, \& 4.6$ keV
(cool for an IP)



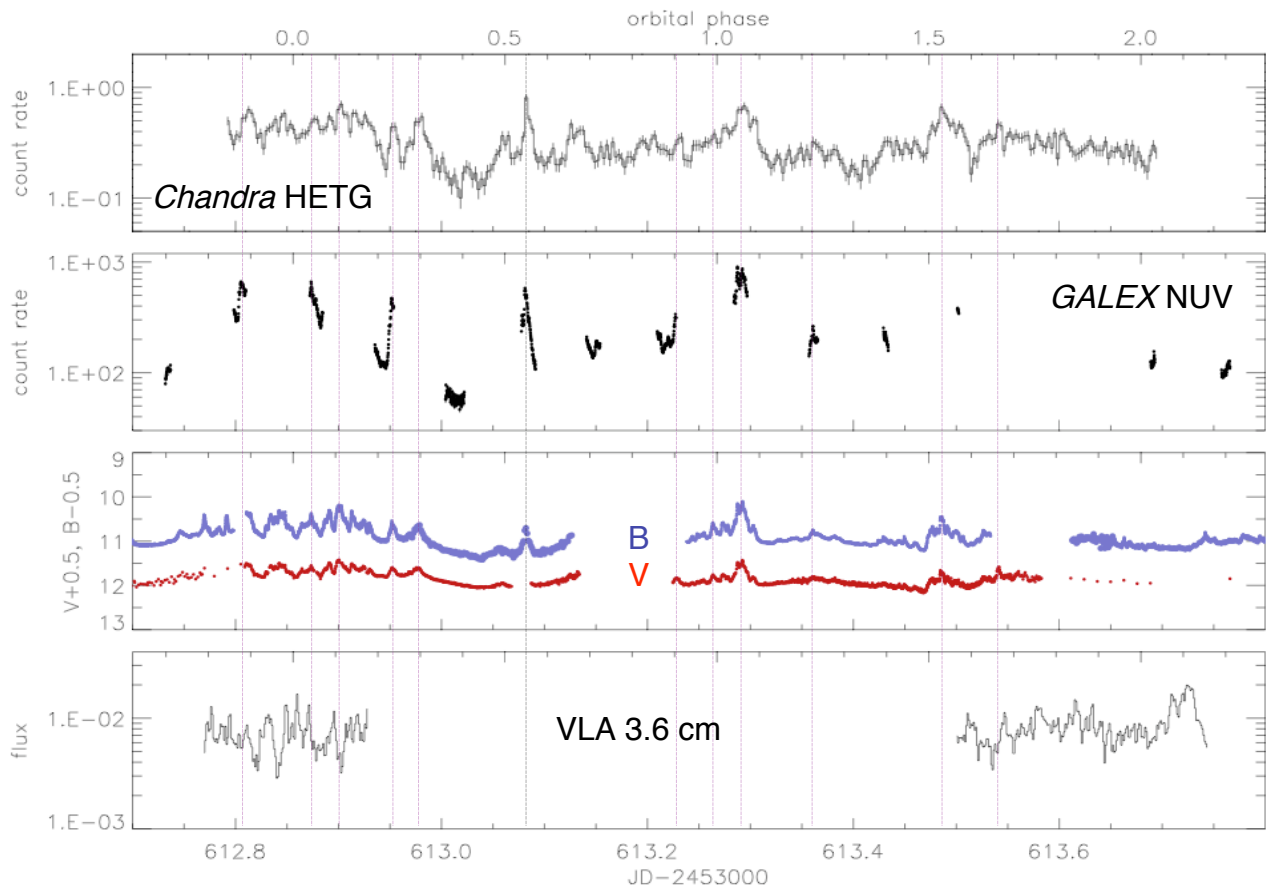
Itoh et al. (2006, ApJ, 639, 397)

He-like N, O, & Ne density diagnostics from the *XMM* RGS spectrum of AE Aqr



$n_e \sim 10^{11} \text{ cm}^{-3}$: low for a magnetic CV

X-ray, UV, optical, & radio light curves of AE Aqr

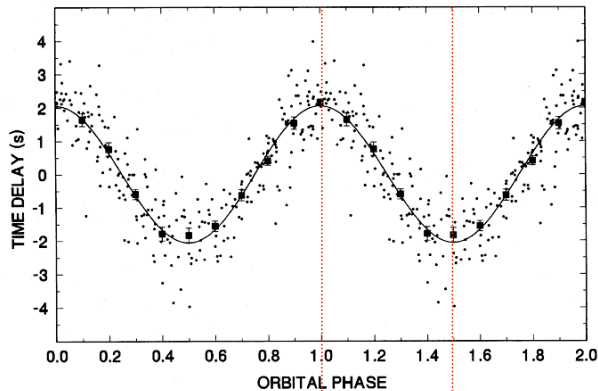


Optical: Ioannou (Skinakas), Welsh (Laguna), CBA, & AAVSO
Radio: Abada-Simon & Desmurs

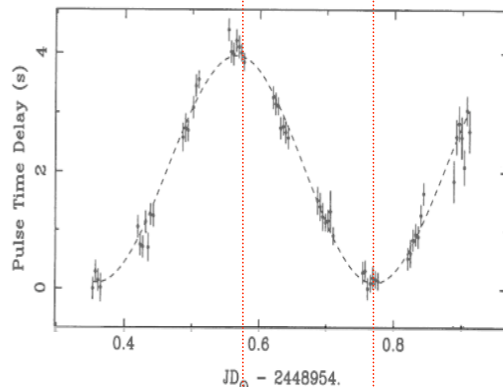
Strong correlation of the flares in the X-ray, UV, and optical, but not in the radio.

Mauche et al. (2007, in preparation)

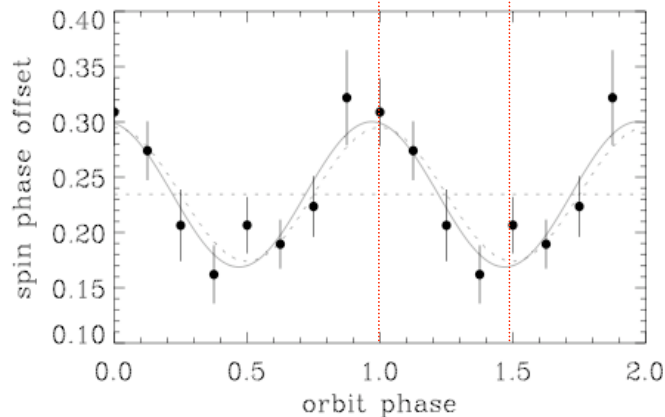
Pulse-timing delays of AE Aqr



Optical:
 $a \sin i = 2.04 \pm 0.13$ s
de Jager et al. (1994)



HST FOS UV:
 $a \sin i = 1.93 \pm 0.03$ s
Eracleous et al. (1994)

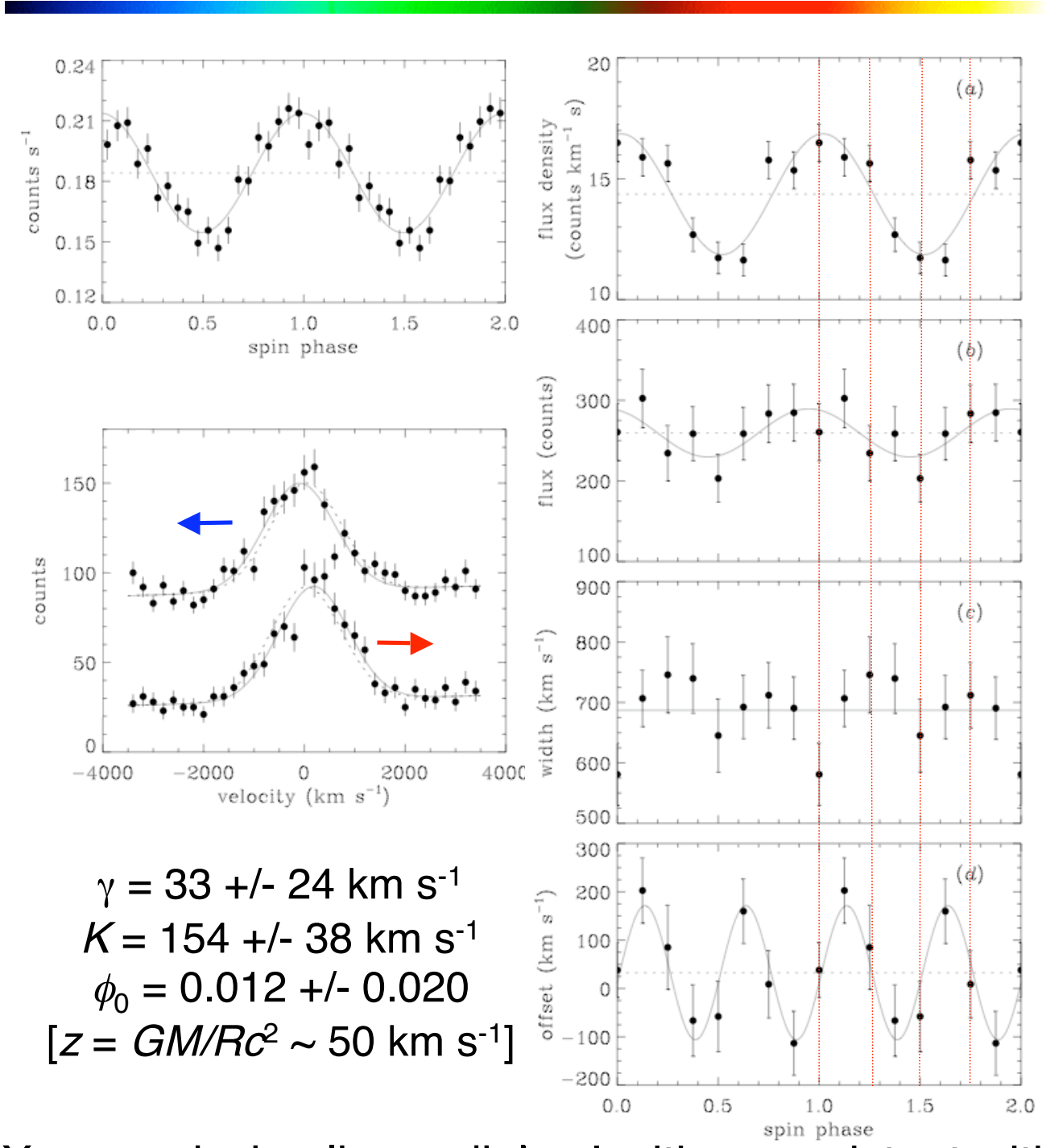


Chandra HETG X-ray:
 $a \sin i = 2.17 \pm 0.48$ s
Mauche (2006)*

Pulsating optical, UV, & X-ray source follows the motion of the white dwarf.

*Mauche (2006, MNRAS, 369, 1983)

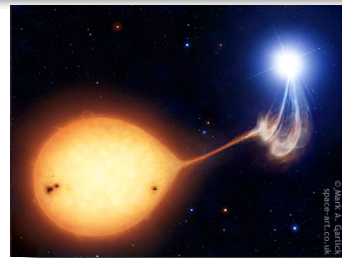
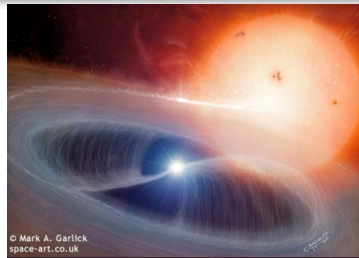
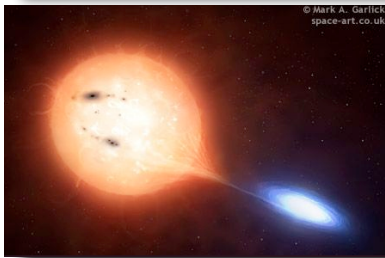
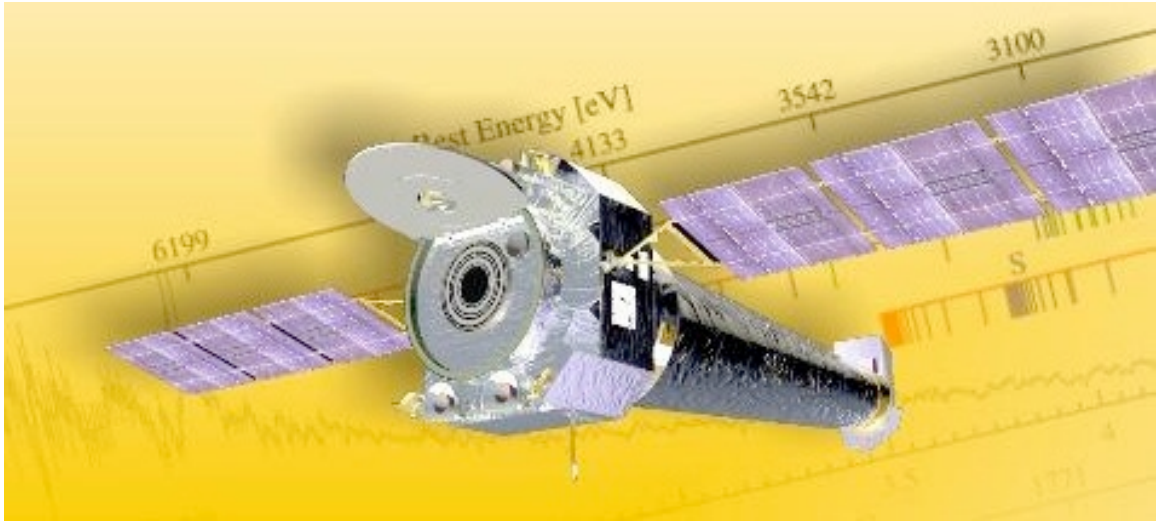
AE Aqr spin-phase light curves and radial velocity variation



$\gamma = 33 \pm 24 \text{ km s}^{-1}$
 $K = 154 \pm 38 \text{ km s}^{-1}$
 $\phi_0 = 0.012 \pm 0.020$
 $[z = GM/Rc^2 \sim 50 \text{ km s}^{-1}]$

X-ray emission line radial velocities consistent with emission from *two* poles. Mauche (2007, in preparation)

Acknowledgements



Support for this work was provided by NASA through *Chandra* Award Number GO5-6021X issued by the *Chandra* X-Ray Observatory Center, which is operated by the Smithsonian Astrophysical Observatory for and on behalf of NASA under contract NAS8-39073. This work was performed under the auspices of the US Department of Energy by the University of California Lawrence Livermore National Laboratory under contract W-7405-Eng-48.